A novel (1,4)-β-linked glucoxylan is synthesized by members of the *cellulose synthase-like F* gene family in land plants

SUPPORTING INFORMATION

Alan Little, Jelle Lahnstein, David W. Jeffery, Shi F. Khor, Julian G. Schwerdt, Neil J. Shirley, Michelle Hooi, Xiaohui Xing, Rachel A. Burton and Vincent Bulone.

Methods

DNA constructs

A mixture of barley tissues, including leaf, root, coleoptile and endosperm, was used to isolate total RNA and generate cDNA using the methods described in Burton, et al. [1]). The full-length cDNA of each member of the barley *CslF* family was amplified as described in [1] using the primers listed in Supplementary Table S1. PCR fragments of the correct size were excised from the gel, purified using NucleoSpin® Gel and PCR Clean-up kit (Machery-Nagel, Amtsgericht Düren, Germany) and inserted into the pCR8/GW/TOPO vector (Life Technologies, Carlsbad, USA) as per the manufacturer's instructions, and sequenced (Australian Genome Research Facility Ltd, Adelaide, Australia). Correct constructs were transferred to the pEAQ-HT-DEST-1 binary expression vector carrying the Gateway™ cloning system [2] using LR Clonase (Life Technologies) as per manufacturer's instructions.

Transient transformation of Nicotiana benthamiana

All *N. benthamiana* plants were grown at 22 °C day and 15 °C night temperatures without supplemental light in the Plant Accelerator® (University of Adelaide). *Agrobacterium tumefaciens* preparation and transformation procedures were adapted from Wydro, et al. [3]). *Agrobacterium* AGL1 harboring the insert and vector of interest were grown with shaking for 48 hours at 28 °C in 10 mL tubes containing 2 mL Luria Broth (LB) supplemented with 50 µg/mL kanamycin and 50 µg/mL rifampicin. An aliquot of 200 µL was spread onto two LB Agar plates supplemented with the same antibiotics and incubated overnight at 28 °C. Agrobacterium was scraped off plates and diluted to an OD600 of 1.0 with minimal media (0.01 M $MgCl_2$ and 0.01 M MES). After incubation for 3 h at room temperature with 0.1 µM acetosyringone, entire intact leaves were infiltrated using a 10 mL syringe without a needle. Tissue was harvested six days post infiltration for analysis.

HvCslF3 and *HvCslF10* transcript profiling was carried out using Q-PCR to confirm expression of the transgene (Supplementary Figure S3).

Measurement of (1,3;1,4)-β-glucan levels

Analysis of (1,3;1,4)-β-glucan content was performed in triplicate for each sample using commercially available reagents (Megazyme International Ireland Ltd, Bray, Ireland) and a scaled down industry-approved protocol [1] based on McCleary and Codd [4]). Tissues were snap frozen, freeze dried, ground with metal ball bearings and 20 mg of ground tissue was weighed into individual tubes. Method modifications included two washes with 1 mL 50% ethanol and two washes with 1 mL 100% ethanol at 97 °C for 10 min to remove sugars and chlorophyll. After lichenase digestion, aliquots were also taken for high performance liquid chromatography (HPLC) analysis of the DP3:DP4 ratios. (1,3;1,4)-β-Glucan is reported as mg (1,3;1,4)-β-glucan per mg freeze-dried matter and expressed as a percentage % (w/w).

Alcohol insoluble residue (AIR)

Alcohol insoluble residues were prepared for each sample by adding 1 mL 70% ethanol to 50–100 mg of ground dried tissue in a 2 mL Eppendorf tube. Each sample was vortexed to mix and heated at 100 °C for 30 min. The sample was cooled to room temperature, centrifuged at 10,000 × g for 5 min, and the supernatant was discarded. Sample residue was washed with 1 mL 70% ethanol at room temperature on a slow rotor for 15 min, centrifuged for 5 min at 10,000 × g, and the supernatant was discarded. This extraction was repeated twice with 100% ethanol and the final AIR samples were dried under vacuum.

Monosaccharide analysis

Transformed *N. benthamiana* leaf AIR samples (10 mg) were hydrolyzed using 1 M sulphuric acid. The samples were heated at 100 °C for 3 hours, cooled to room temperature, and stored at −20 °C. Oligosaccharide fractions were hydrolyzed using 2 M trifluoroacetic

acid (TFA), at 100 °C for 3 hours. Hydrolysates were dried under vacuum then dissolved in a suitable volume of water. Monosaccharide analysis of hydrolysate solutions was carried out as per Comino, et al. [5]). Appropriately diluted hydrolysates (10 µL) were derivatized with 1-phenyl-3-methyl-5-pyrazolone (PMP) along with the same volume of a suitable set of calibration standards. Derivative solutions were analyzed using reversed phase HPLC [5].

Driselase hydrolysis, oligosaccharide fractionation and analysis

Driselase treatment was based on the method of Gardner, et al. [6]). AIR samples (10 mg) in 2 mL Eppendorf tubes were digested in a 1 mL volume containing 5 mg/mL partially purified Driselase, 5 mg/mL chlorobutanol, and 20 mM sodium acetate pH 4.8. Hydrolytic reactions were allowed to proceed for 40 h at room temperature with mixing on a slow rotor. Enzymes were inactivated by heating at 100 °C for 10 min. Once cooled to room temperature, samples were centrifuged at 10,000 × g for 5 min. Clarified solutions were analyzed using HPAEC-PAD after dilution with water or oligosaccharides were fractionated from the clarified digests on graphitized carbon SPE cartridges (1 mL / 50 mg, Bond Elute, Agilent Technologies). A 500 µL aliquot of digest solutions was loaded onto cartridges that were pre-conditioned with 1 mL acetonitrile (MeCN), then 1 mL water. The cartridges were washed with 500 µL water and eluted with 500 µL 55% MeCNaq.

Oligosaccharides of interest, Unknown 1 and 2, were purified by HPLC on a carbon column (Hypercarb 5 µm 100 × 4.6 mm, Thermo Fisher Scientific). The column was maintained at 20 °C with a flow rate of 1.0 mL/min. Separation was performed with 10 mM ammonium hydroxide (eluent A) and 90% aqueous MeCN (eluent B) in a gradient of 0 to 20% eluent B over 18 min. The column eluent flow was split with a ratio of 9 (collect):1 (detect). Elution was monitored with evaporative light scattering detection (ELSD model 800, Alltech) operated at 70 °C with a nitrogen pressure of 3 bar and a gain of 8. Unknown-

3, the hydrolysis product of Unknown 1 and 2, was purified in the same way, but using elution with 100% A for 5 min followed by a 4 min gradient to 10% B.

Fractions were analyzed using high pH anion exchange chromatography with pulsed amperometric detection (HPAEC-PAD) on a Dionex ICS-5000 (Thermo Fisher Scientific, Waltham MA, USA) operated as per Ermawar, et al. [7]). Separation was on a Dionex CarboPac PA-20 (3 × 150 mm) column with guard of the same material using 0.1 M NaOH (eluent A) and 0.1 M NaOH with 1 M sodium acetate (eluent B) with a gradient of 1-15% B over 20 min, followed by 100% B for 1 min, and re-equilibration.

Hydrolysates of Unknown 1 and 2 were analysed using high pH anion exchange chromatography as described above, and also using a different gradient: eluent C was 20 mM NaOH, and eluent D was 20 mM NaOH with 200 mM sodium acetate. The first 5 min were isocratic C, then a linear gradient to 100% D over 15 min, followed by 100% B as above, and re-equilibration.

Determination of molecular masses for Unknown 1 and 2

A ThermoFinnigan Surveyor HPLC connected to a ThermoFinnigan LCQ Deca XP Plus mass spectrometer was used with electrospray ionization (ESI) in negative ion mode. Data acquisition and processing was performed using Xcalibur software (version 1.3). Nitrogen was used for sheath gas at 20 arbitrary units, and the capillary temperature was maintained at 250 °C. The ion spray voltage, capillary voltage, and tube lens offset voltage were respectively set as follows for negative ion mode: 4500 V, 40 V, 55 V; −4000 V, −30 V, −35 V. Helium was used as the collision gas for full scan MS/MS experiments targeting *m*/*z* 357 and 327 in negative mode, and *m*/*z* 305 in positive mode. Normalized collision energy, activation Q, activation time and isolation width were 23-30%, 0.250, 30 ms and m/z 1.4-1.7, respectively. A syringe pump operating at 5 µL/min was used to infuse sample into an LC flow of 0.100 mL/min with 0.5% aqueous formic acid as the eluent.

Determination of high resolution molecular mass of gluconic acid

The analysis was performed on an Agilent 1200 SL HPLC coupled to a Bruker microTOF-Q II. The following MS parameters were set: ESI negative; source temperature, 200 °C; capillary voltage, 3500 V; end plate offset -500 V, nebulizer pressure 2 Bar, dry gas flow 7 L/min, mass range *m*/*z* 50-1650, acquisition rate 0.5 Hz, calibration solution 5 mM sodium hydroxide, 0.2% formic acid in 50% 2-propanol. A mass calibration was applied to the sample via the calibration mix being run at the end of the analysis. The predicted molecular formula was based upon a 2 mDa error tolerance and carbon, hydrogen, oxygen and nitrogen were considered.

Cellulase hydrolysis, oligosaccharide fractionation and analysis

Endo-glucanase (endo-(1,4)-β-D-glucanohydrolase, EC 553 3.2.1.4) from *Aspergillus niger* (E-CELAN) or *Trichoderma longibrachiatum* (E-CELTR), Megazyme) digest conditions for AIR samples were the same as those used for Driselase digests: 5U of enzyme was used per reaction and the time of hydrolysis was limited to overnight [8]. A larger scale digest was carried out to allow preparative fractionation of oligosaccharides Unknown 3 and 4. Clarified hydrolysates and/or a Carbon SPE oligosaccharide fraction were analyzed using HPAEC-PAD. Conditions were as above with the following gradient: A = 0.1 M NaOH, B = 0.1 M NaOH/1 M sodium acetate, C = 20 mM NaOH, isocratic elution with C for 5 min, a linear gradient to A over 15 min, a linear gradient to 15% B over 10 min, then a 100% B for 1 min, and re-equilibration.

Unknown 3 and 4 were purified using aqueous normal phase chromatography on a Prevail Carbohydrate ES column (Alltech, 150 × 4.6 mm, 5 μm). A = water, B = 90% acetonitrile, flow rate was 1.0 mL/min, temperature was 20 °C, the gradient was 94.5 to 80% B over 18 min, followed by 80% water flush for 1 min, and re-equilibration. The column eluent flow was split with a ratio of 9 (collect):1 (detect). Elution was monitored with evaporative light

scattering detection (ELSD model 800, Alltech) operated at 70 °C with a nitrogen pressure of 3 bar and a gain of 8. Fractions were analyzed using HPAEC-PAD.

Purified oligosaccharide solution concentrations were determined using monosaccharide analysis. The oligosaccharides were characterized using methylation linkage analysis and Nuclear magnetic resonance spectroscopy (NMR). These solutions were also then used as standards to quantitate the amount of XG and GX released from native barley tissues and to confirm their structures by LC-MS^2 as their PMP derivatives.

Two fractions of oligosaccharides eluting after XG and GX on HPAEC-PAD were prepared using Carbon SPE (Bond Elut 1mL / 50mg Agilent Technologies, Singapore). Monosaccharides and disaccharides were eluted with acetonitrile in water up to 10%, then 15% acetonitrile and 55% acetonitrile fractions were collected containing the larger oligosaccharides. These fractions were analyzed using HPAEC-PAD, monosaccharide analysis, and LC-MS^2 as their PMP derivatives.

Polysaccharide fractionation

An AIR preparation of 2 × 125 mg *N. benthamiana* leaf transformed with *HvCslF10* was carried out in 50 mL tubes. The pellets were washed with water and then sequentially extracted with a series of solvents as follows: water at 100 °C, DMSO at 50 and 100 °C, and DMSO with 2, 6, and 20% EmimAc all at 60 °C. Extractions of 30 min (2 × 10 mL) were undertaken with each solvent, with mixing at the start and at 15 and 30 min. Samples were centrifuged at 3220 × g for 5 min and extracts of the same solvent were pooled and precipitated with 80% ethanol. Monosaccharide analysis of the fractions and analysis for glucoxylan content by digestion with E-CELTR and HPAEC-PAD was carried out.

Glycosidic linkage analysis

Separate samples of Unknown 3 and 4 were per-methylated [9], followed by trifluoroacetic acid (TFA) hydrolysis, reduction with $NaBD_4$, and per-acetylation with acetic anhydride to generate partially methylated alditol acetates (PMAAs) [10]. The PMAAs were separated using gas chromatography as described earlier [11-12] except that an Agilent J&W VF-23ms capillary column (30 m × 0.25 mm i.d.) was used for the separation of PMAAs on an Agilent 7890B/5977B GC-MS system coupled with flame ionization detection (FID). The PMAAs were identified by comparing their MS fragmentation patterns with those of reference derivatives and by referring to the literature [13], and quantified based on the FID response [13-14]. Experiments were conducted in duplicate.

^{13}C-Nuclear magnetic resonance spectroscopy (NMR)

^{13}C-NMR data were collected on an Agilent 600 MHz DD2 NMR system equipped with a ^{13}C enhanced cryoprobe on samples dissolved in deuterated water. The software used was VnmrJ software version 4.2 with default parameters including a frequency of 150 MHz, a 60 degree pulse and a relaxation delay of 2 s.

Liquid chromatography/tandem mass spectrometry of PMP derivatives of Unknown 3, Unknown 4 and fractions containing larger oligosaccharides

Analysis was performed using an ultra-performance liquid chromatography system (UPLC) coupled to a 6545 quadrupole time of flight (qTOF) mass spectrometer (Agilent Technologies, Singapore) fitted with a C18 reverse phase column (100 × 2.1 mm, 1.8 μm particle size, Agilent Technologies, Santa Clara, California) and a guard column of the same material. The analytes were separated at 30 °C with a flow rate of 0.4 mL/ min using 15 to 25% acetonitrile in water with 0.1% formic acid.

The UPLC was connected to the mass spectrometer via a dual Agilent Jetstream electrospray interface (Dual AJS ESI). A capillary voltage of 4 kV was applied. The source

gas temperature was 325 °C with a flow rate of 8 L/ min and sheath gas was 400 °C with a flow rate of 10 L/ min. The qTOF was operated in both high resolution positive and negative ion modes. Data dependent acquisition of mass spectra with a full scan (m/z = 100-1500) were accomplished in centroid mode. The top three precursor ions were selected and further fragmented using nitrogen as the collision gas (40 eV for the disaccharides and 35 eV for the larger oligosaccharides). The precursor ion was isolated with an isolation width of 1.3 Da. Purine and hexakis were used as reference lock-mass compounds with automatic mass correction enabled. The masses observed in positive mode were m/z = 121.0590 and m/z = 922.0098. The mass correction was operated using the Agilent Mass Hunter Qualitative software (B.01.03 version). The QTOF was tuned and calibrated using the ESI-low concentration tuning mix (Agilent Technologies, Santa Clara, USA).

Peak lists were generated using the Agilent Technologies MassHunter Workstation software for 6545 Series TOF. The results were reviewed and manually curated. The MS^2 spectra were used to confirm the identity of the compounds based on the m/z values of their typical fragments.

Reverse-transcription quantitative PCR (Q-PCR) of HvCslF3 *and* HvCslF10 *transcripts*

Total RNA was isolated from 7 day old barley tissues using the Spectrum™ Plant Total RNA Kit (Sigma-Aldrich, St Louis, U.S.A.) following the manufacturer's protocol. cDNA was synthesized from total RNA using SuperScript® III Reverse Transcriptase (RT) enzyme (Life Technologies, Carlsbad, U.S.A.) following the recommended protocol. *HvCslF3* and *HvCslF10* transcript profiling was carried out using Q-PCR as described previously in Burton *et al.* [1] using the gene-specific primers in Supplementary Table S1. The data were normalized against the geometric mean of the four control genes, namely glyceraldehyde 3-phosphate dehydrogenase (GAPDH), cyclophilin, tubulin and HSP70 [15].

Phylogenetic analysis

CslF coding sequences were sampled using matches to the PF03552 PFAM (Finn et al., 2016) from Phytozome [16] and Ensembl [17]. Sequences were aligned using MUSCLE [18] and edited for significant error with BMGE using unstringent parameters (-m BLOSUM30, -g 0.7, -b 2). A best-known maximum likelihood tree was constructed with RAxML version 8.2.4 (Stamatakis, 2014) using the GTRGAMMA substitution model. We used Treefix [19] to correct for the lack of information in a single locus gene tree. Support values and branch lengths were calculated in RAxML and applied to the Treefix adjusted topology. DLCpar [20] was used to reconcile the species and gene trees to determine the gene duplication and loss history. Tests for episodic selection were performed using BUSTED as implemented in HYPHY [21].

References

1. Burton, R. A.; Collins, H. M.; Kibble, N. A. J.; Smith, J. A.; Shirley, N. J.; Jobling, S. A.; Henderson, M.; Singh, R. R.; Pettolino, F.; Wilson, S. M.; Bird, A. R.; Topping, D. L.; Bacic, A.; Fincher, G. B. Over-expression of specific *HvCslF cellulose synthase-like* genes in transgenic barley increases the levels of cell wall (1,3;1,4)-β-d-glucans and alters their fine structure. *Plant Biotechnology Journal* **2010,** *9* (2), 117-135.
2. Sainsbury, F.; Thuenemann, E. C.; Lomonossoff, G. P. pEAQ: versatile expression vectors for easy and quick transient expression of heterologous proteins in plants. *Plant Biotechnology Journal* **2009,** *7* (7), 682-693.
3. Wydro, M.; Kozubek, E.; Lehmann, P. Optimization of transient Agrobacterium-mediated gene expression system in leaves of *Nicotiana benthamiana*. *Acta Biochimica Polonica* **2006,** *53* (2), 289-298.
4. McCleary, B. V.; Codd, R. Measurement of (1,3;1,4)-β-D-glucan in barley and oats a streamlined enzymic procedure. *Journal of Science Food Agriculture* **1991,** *55*, 303-312.
5. Comino, P.; Shelat, K.; Collins, H.; Lahnstein, J.; Gidley, M. J. Separation and purification of soluble polymers and cell wall fractions from wheat, rye and hull less barley endosperm flours for structure-nutrition studies. *Journal of Agricultural and Food Chemistry* **2013,** *61* (49), 12111-12122.
6. Gardner, S. L.; Burrell, M.; Fry, S. C. Screening of *Arabidopsis thaliana* stems for variation in cell wall polysaccharides. *Phytochemistry* **2002,** *60* (3), 241-254.
7. Ermawar, R. A.; Collins, H. M.; Byrt, C. S.; Betts, N. S.; Henderson, M.; Shirley, N. J.; Schwerdt, J.; Lahnstein, J.; Fincher, G. B.; Burton, R. A. Distribution, structure and

biosynthetic gene families of (1, 3; 1, 4)-β-glucan in *Sorghum bicolor*. *Journal of Integrative Plant Biology* **2015,** *57* (4), 429-445.
8. Roberts, A. W.; Lahnstein, J.; Hsieh, Y. S.; Xing, X.; Yap, K.; Chaves, A. M.; Scavuzzo-Duggan, T. R.; Dimitroff, G.; Lonsdale, A.; Roberts, E. M. Functional characterization of a glycosyltransferase from the moss *Physcomitrella patens* involved in the biosynthesis of a novel cell wall arabinoglucan. *The Plant Cell* **2018**, tpc. 00082.2018.
9. Ciucanu, I.; Kerek, F. A simple and rapid method for the permethylation of carbohydrates. *Carbohydrate Research* **1984,** *131* (2), 209-217.
10. Pettolino, F. A.; Walsh, C.; Fincher, G. B.; Bacic, A. Determining the polysaccharide composition of plant cell walls. *Nature Protocols* **2012,** *7* (9), 1590-1607.
11. Mélida, H.; Sandoval-Sierra, J. V.; Diéguez-Uribeondo, J.; Bulone, V. Analyses of extracellular carbohydrates in oomycetes unveil the existence of three different cell wall types. *Eukaryotic Cell* **2013,** *12* (2), 194-203.
12. Mélida, H.; Sain, D.; Stajich, J. E.; Bulone, V. Deciphering the uniqueness of Mucoromycotina cell walls by combining biochemical and phylogenomic approaches. *Environmental Microbiology* **2015,** *17* (5), 1649-1662.
13. Carpita, N. C.; Shea, E. M. Linkage structure of carbohydrates by gas chromatography-mass spectrometry (GC-MS) of partially methylated alditol acetates. *Analysis of Carbohydrates by GLC and MS* **1989**, 157-216.
14. Sweet, D. P.; Shapiro, R. H.; Albersheim, P. Quantitative analysis by various GLC response-factor theories for partially methylated and partially ethylated alditol acetates. *Carbohydrate Research* **1975,** *40* (2), 217-225.
15. Vandesompele, J.; De Preter, K.; Pattyn, F.; Poppe, B.; Van Roy, N.; De Paepe, A.; Speleman, F. Accurate normalization of real-time quantitative RT-PCR data by geometric averaging of multiple internal control genes. *Genome Biology* **2002,** *3* (7), research0034.1 - research0034.12.
16. Goodstein, D. M.; Shu, S.; Howson, R.; Neupane, R.; Hayes, R. D.; Fazo, J.; Mitros, T.; Dirks, W.; Hellsten, U.; Putnam, N.; Rokhsar, D. S. Phytozome: a comparative platform for green plant genomics. *Nucleic acids research* **2012,** *40* (Database issue), D1178-86.
17. Zerbino, D. R.; Achuthan, P.; Akanni, W.; Amode, M. R.; Barrell, D.; Bhai, J.; Billis, K.; Cummins, C.; Gall, A.; Girón, C. G. Ensembl 2018. *Nucleic acids research* **2017,** *46* (D1), D754-D761.
18. Edgar, R. C. MUSCLE: multiple sequence alignment with high accuracy and high throughput. *Nucleic acids research* **2004,** *32* (5), 1792-7.
19. Wu, Y.-C.; Rasmussen, M. D.; Bansal, M. S.; Kellis, M. TreeFix: statistically informed gene tree error correction using species trees. *Systematic Biology* **2012,** *62* (1), 110-120.

20. Wu, Y.-C.; Rasmussen, M. D.; Bansal, M. S.; Kellis, M. Most parsimonious reconciliation in the presence of gene duplication, loss, and deep coalescence using labeled coalescent trees. *Genome Research* **2014,** *24* (3), 475-486.
21. Murrell, B.; Weaver, S.; Smith, M. D.; Wertheim, J. O.; Murrell, S.; Aylward, A.; Eren, K.; Pollner, T.; Martin, D. P.; Smith, D. M. Gene-wide identification of episodic selection. *Mol Biol Evol* **2015,** *32* (5), 1365-1371.

Supplementary Table S1: Primers used for cloning full-length cDNA of *HvCslF* family members.

Primer name	Sequence
HvCslF3-fQPCR	CTTGTTGCCGGTTGCCTTTACA
HvCslF3-rQPCR	TCAATTGGCTAAAATGGAAGAAAACTA
HvCslF10-fQPCR	GGCTATTGTTCAACCTGTGGATTA
HvCslF10-rQPCR	TGGCCAAGAAAGCAATGGGTAGT
HvCslF3-F	CGGTCGGGAAACCTGGGAGTGG
HvCslF3-R	GGTACAAAGTACAAGTACTACAATGG
HvCslF4-F	GCACGTAGGCACTTACACTATGG
HvCslF4-R	TTGCAGTGACTCTGGCTGTACTTG
HvCslF6-F	ACGGCCATGGCGCCAGCGGTGGC
HvCslF6-R	TGTCCGGGCAAAGTCATCAA
HvCslF7-F	ATGTTAATGACATATATCACC
HvCslF7-R	TTAAAGCATATGCAAATGGAG
HvCslF8-F	GTAGCTGGCTACTGTGCATAGC
HvCslF8-R	GCTGTTGCTTTGCCACATCTC
HvCslF9-F	CTCTGCTACTTGGTAGGCGGACC
HvCslF9-R	AGGTTTTGCAGCATTACTTGA
HvCslF10-F	CGTGGTTGATGATTGCAATCC
HvCslF10-R	GTTCAACTACATAAGTCCC

Supplementary Figure S1: MS fragmentation pattern of partially methylated alditol acetate (PMAA) from the t-Xyl*p* in the disaccharide Xyl*p*-(1,4)-Glc*p* (S1A), the 4-Glc*p* in the disaccharide Xyl*p*-(1,4)-Glc*p* (S1B), the t-Glc*p* in the disaccharide Glc*p*-(1,4)-Xyl*p* (S1C) and the 4-Xyl*p* in the disaccharide Glc*p*-(1,4)-Xyl*p* (S1D).

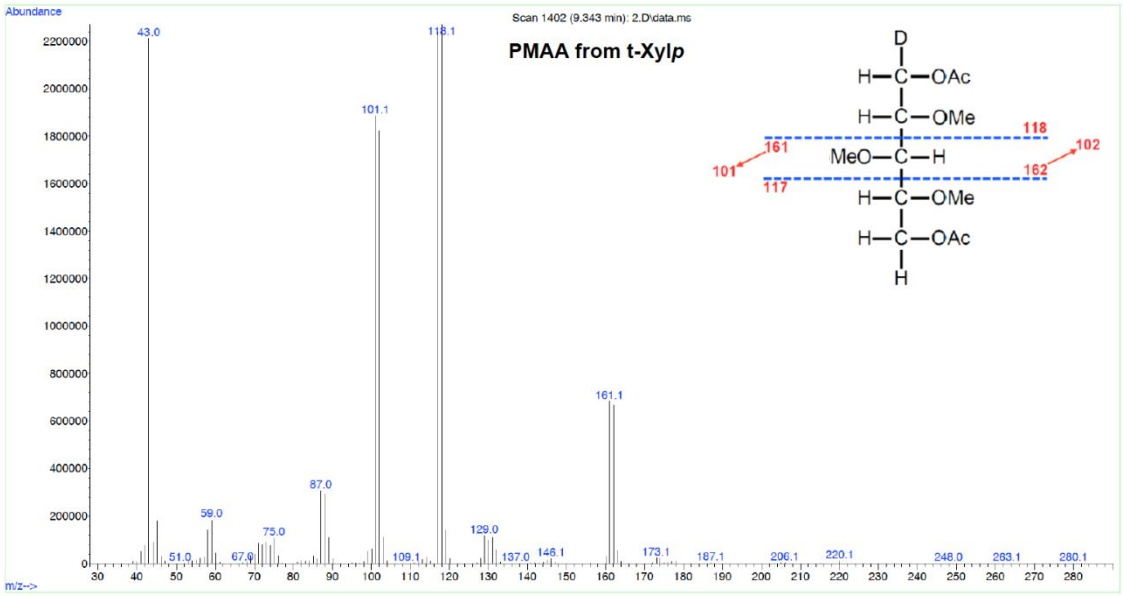

Figure S1A. MS fragmentation pattern of partially methylated alditol acetate (PMAA) from the t-Xyl*p* in the disaccharide Xyl*p*-(1,4)-Glc*p*

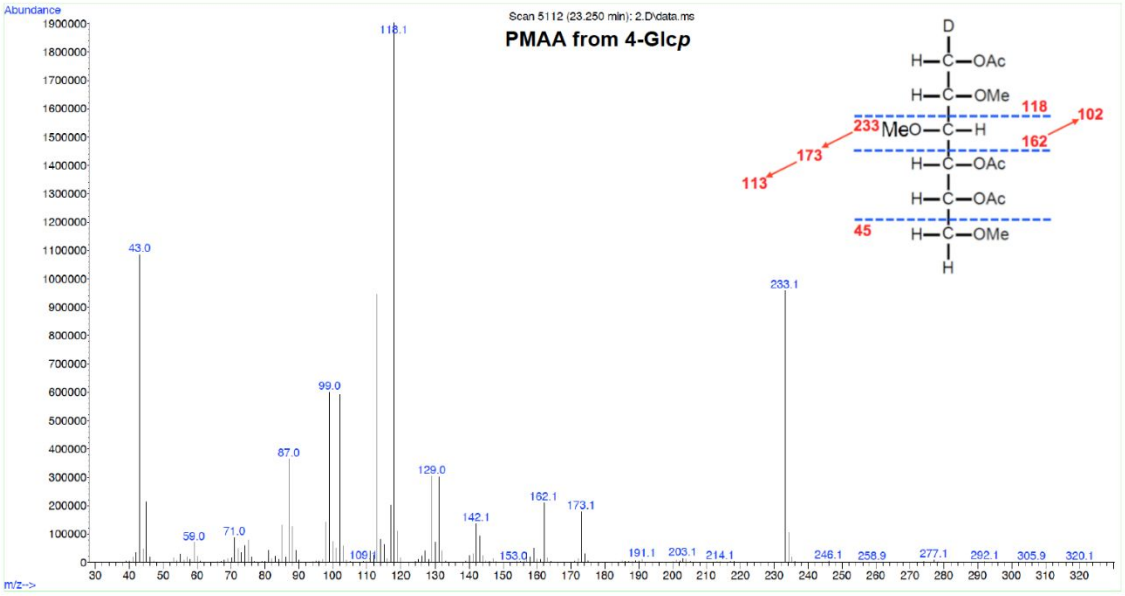

Figure S1B. MS fragmentation pattern of partially methylated alditol acetate (PMAA) from the 4-Glc*p* in the disaccharide Xyl*p*-(1,4)-Glc*p*

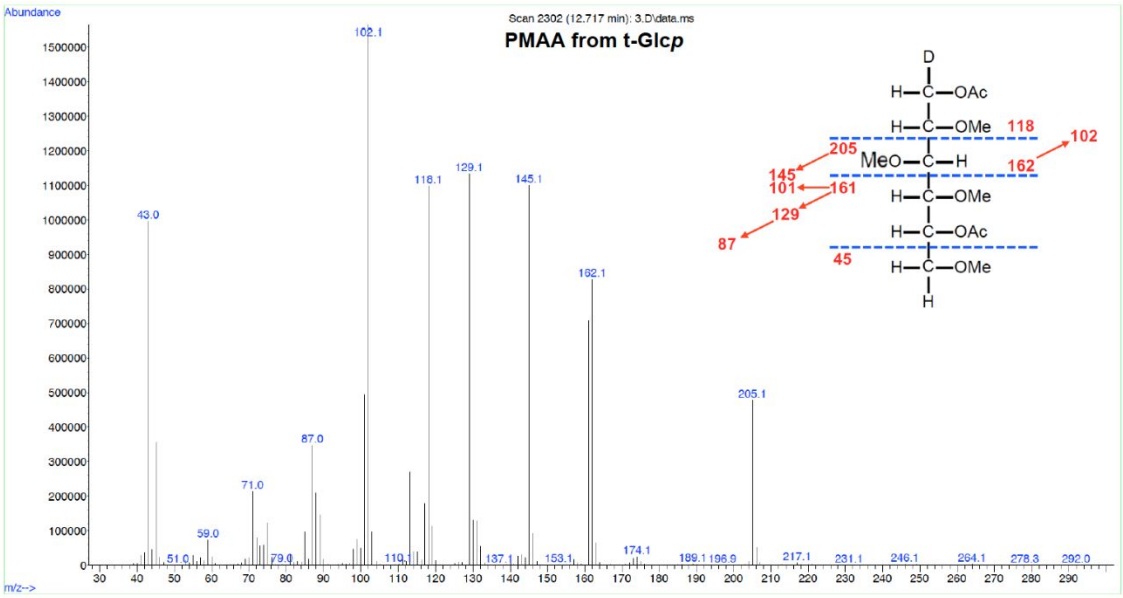

Figure S1C. MS fragmentation pattern of partially methylated alditol acetate (PMAA) from the t-Glc*p* in the disaccharide Glc*p*-(1,4)-Xyl*p*

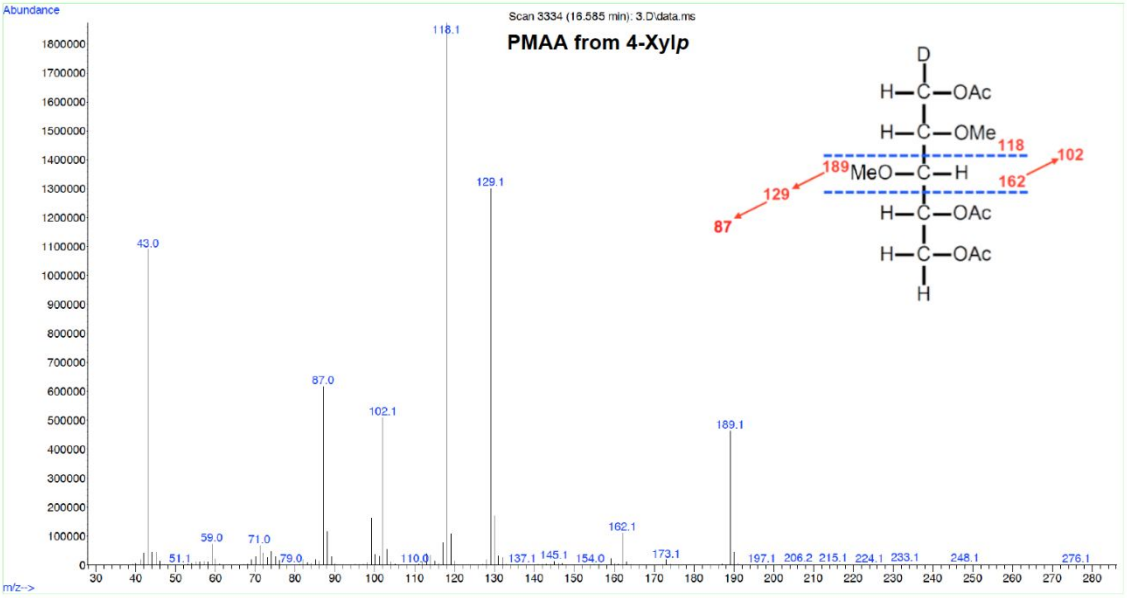

Figure S1D. MS fragmentation pattern of partially methylated alditol acetate (PMAA) from the 4-Xyl*p* in the disaccharide Glc*p*-(1,4)-Xyl*p*

Supplementary Figure S2: LC-TOF MS analysis of PMP labeled Glc-(1,4)-β-Xyl (S2A-C) and Xyl-(1,4)-β-Glc (S2D-F) disaccharide standards. LC-TOF MS analysis of oligosaccharides produced post-cellulase (E-CELTR) hydrolysis of 7 day old barley seedling tissues naturally expressing *HvCslF3* and *HvCslF10* including; Leaf (S2G-I), Coleoptile (S2J-L), Upper roots (S2M-O), Mid roots (S2P-R) and Root tips (S2S-U). LC-TOF MS analysis of oligosaccharides produced post-cellulase (E-CELTR) hydrolysis of *N. benthamiana* tissues overexpressing a negative control infiltrated with Agrobacterium containing an empty expression vector (S2V-X), *HvCslF3* (S2Y-AA) and *HvCslF10* (S2BB-DD).

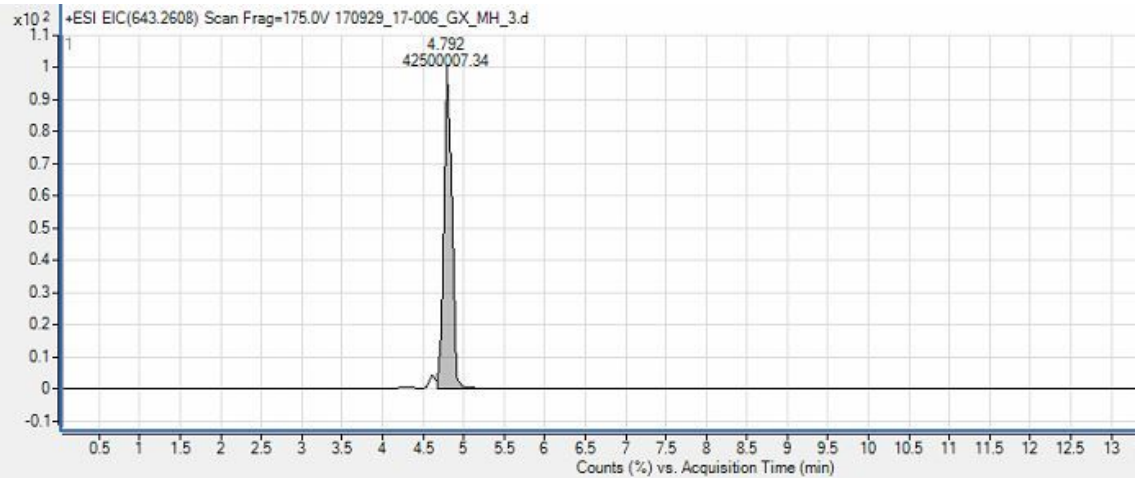

Figure S2A. Extracted ion chromatogram (EIC) of PMP labeled Glc-(1,4)-β-Xyl disaccharide.

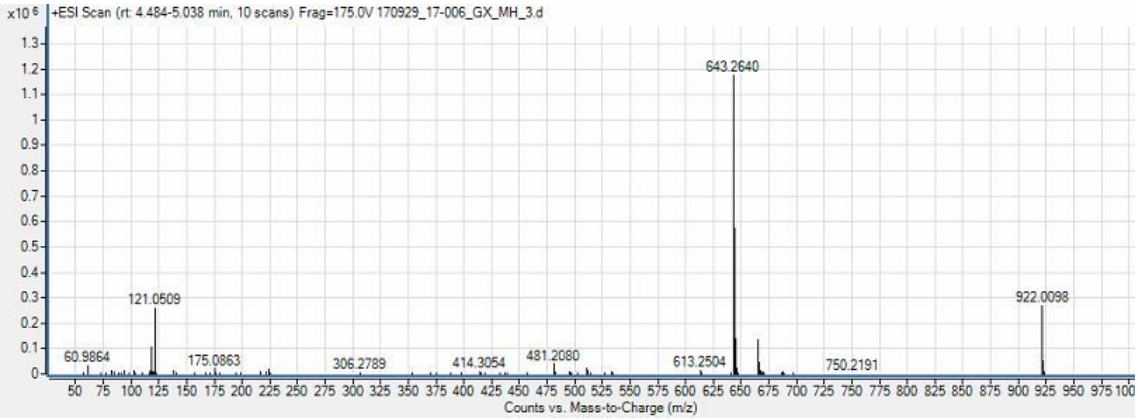

Figure S2B. Positive ESI-MS2 spectra of the $[M+ H]^+$ of PMP labelled Glc-(1,4)-β-Xyl disaccharide.

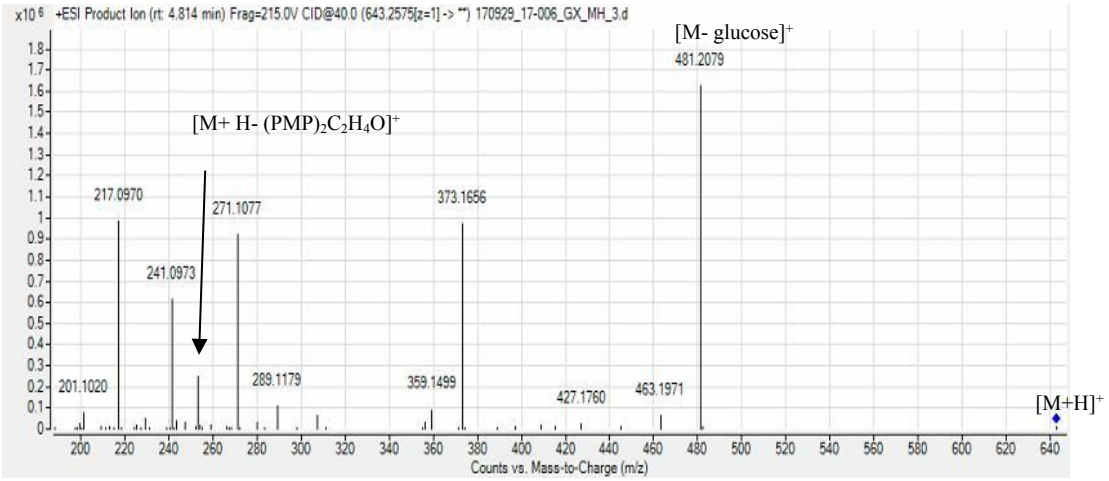

Figure S2C. Positive ESI-MS2 spectra of the $[M+ H]^+$ of PMP labeled Glc-(1,4)-β-Xyl disaccharide.

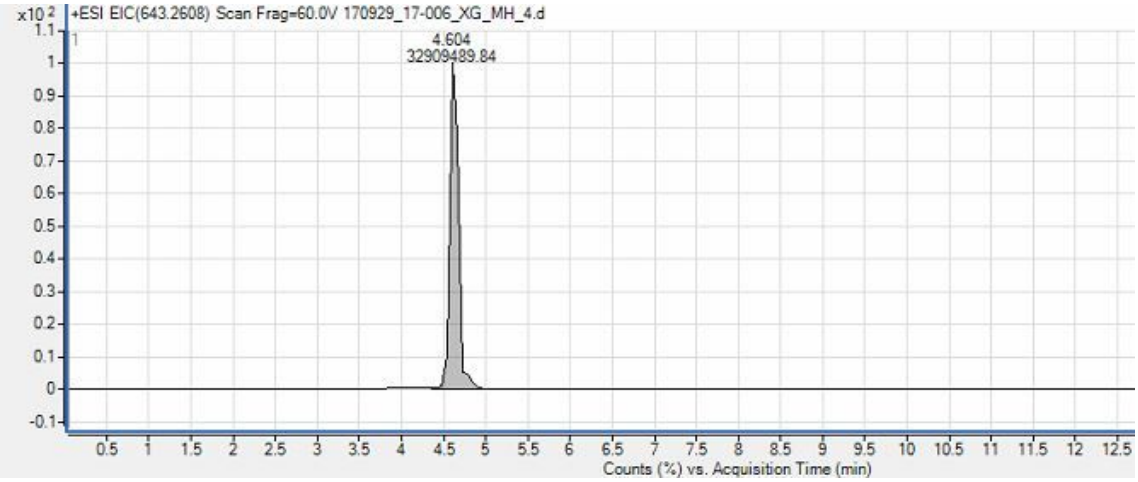

Figure S2D. Extracted ion chromatogram (EIC) of PMP labeled Xyl-(1,4)-β-Glc disaccharide.

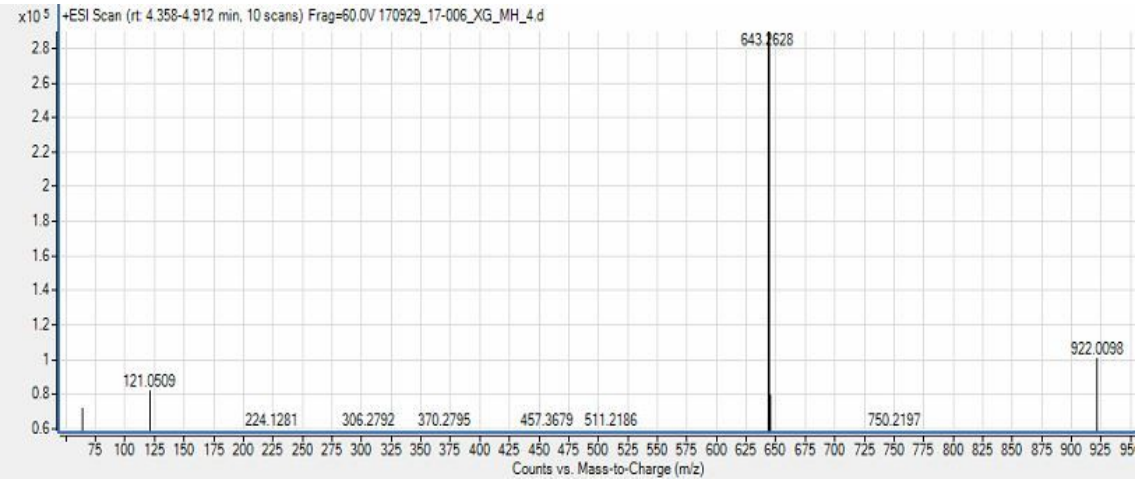

Figure S2E. Positive ESI-MS2 spectra of the $[M+ H]^+$ of PMP labeled Xyl-(1,4)-β-Glc disaccharide.

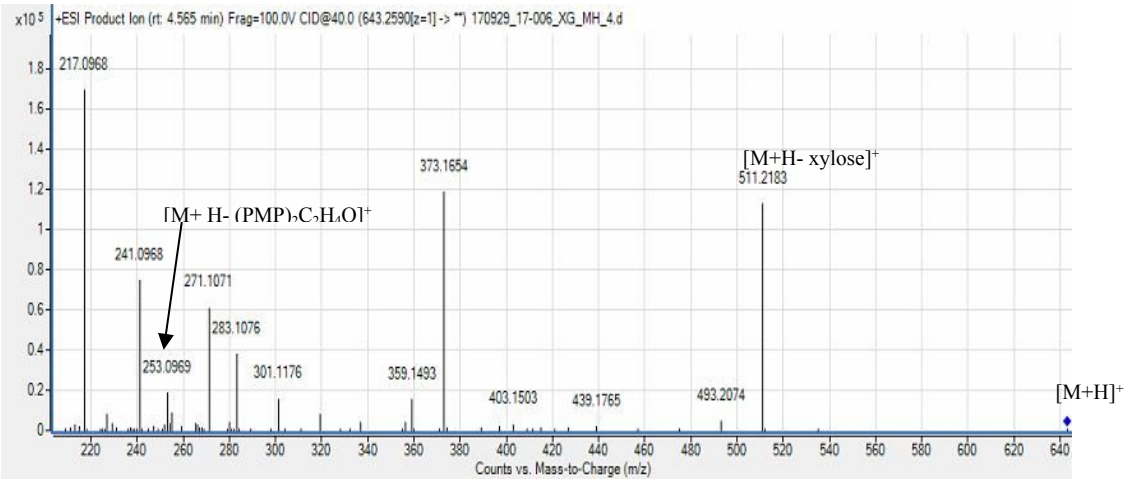

Figure S2F. Positive ESI-MS2 spectra of the [M+ H]$^+$ of PMP labeled Xyl-(1,4)-β-Glc disaccharide.

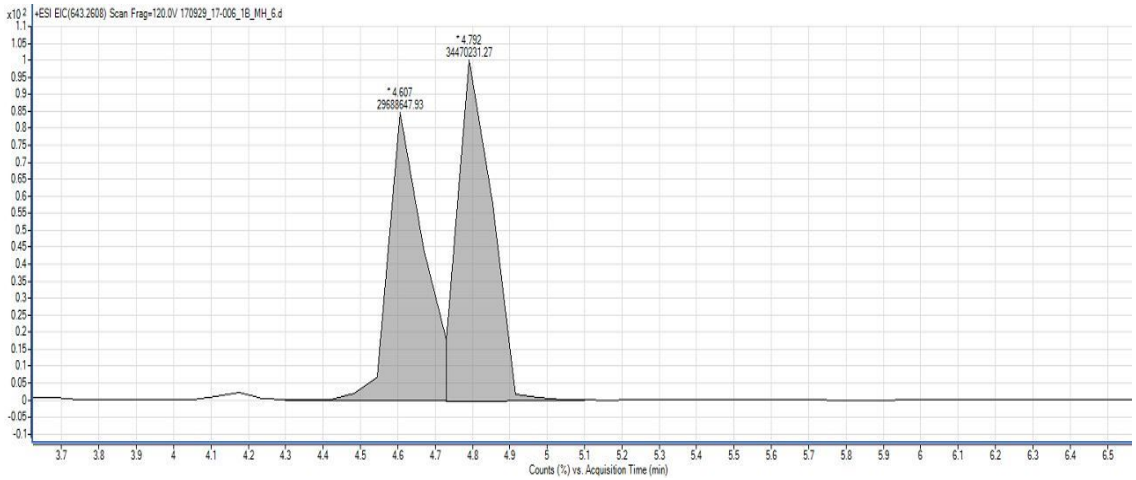

Figure S2G. Extracted ion chromatogram (EIC) of Barley Leaf.

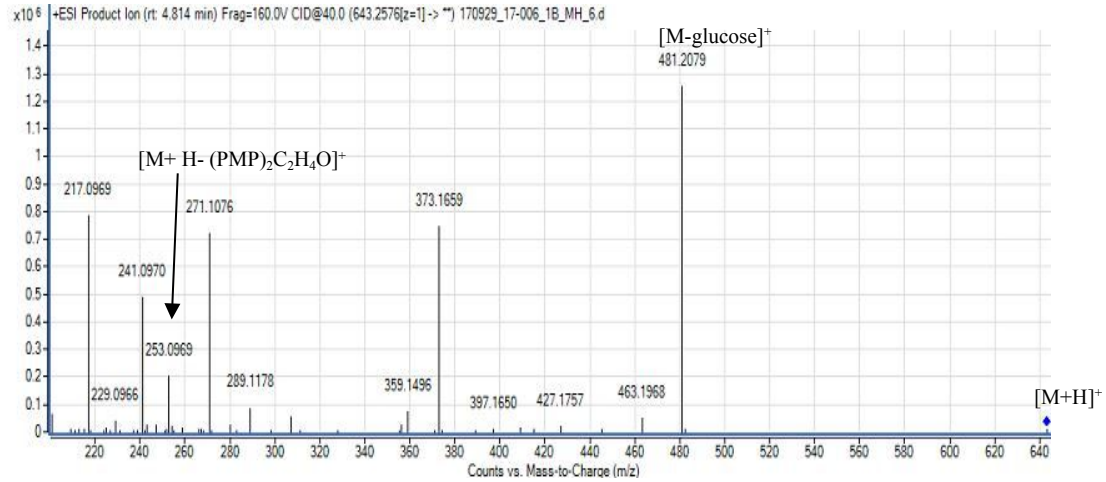

Figure S2H. Positive ESI-MS2 spectra of the [M+ H]$^+$ of PMP labeled Glc-(1,4)-β-Xyl disaccharide in Barley Leaf.

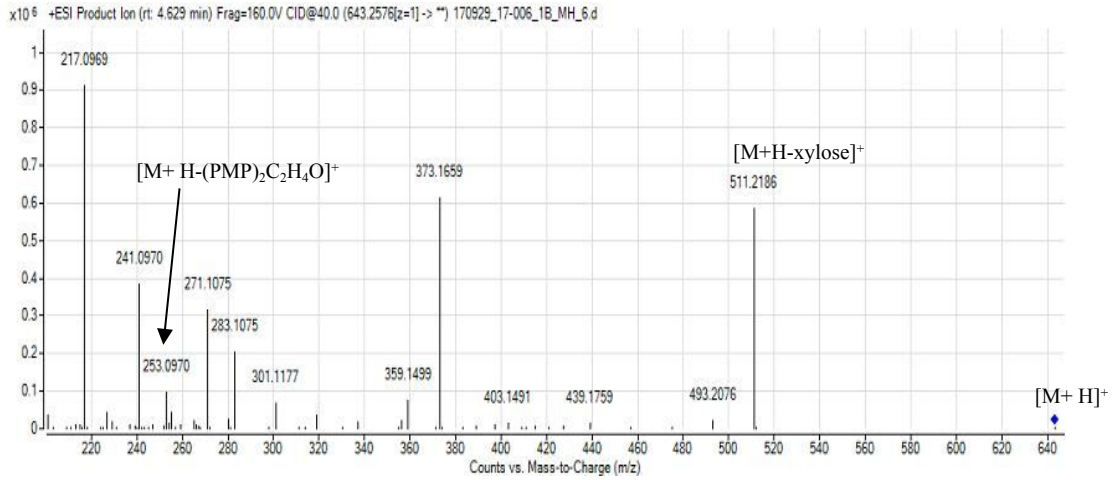

Figure S2I. Positive ESI-MS2 spectra of the $[M+ H]^+$ of PMP labeled Xyl-(1,4)-β-Glc disaccharide in Barley Leaf.

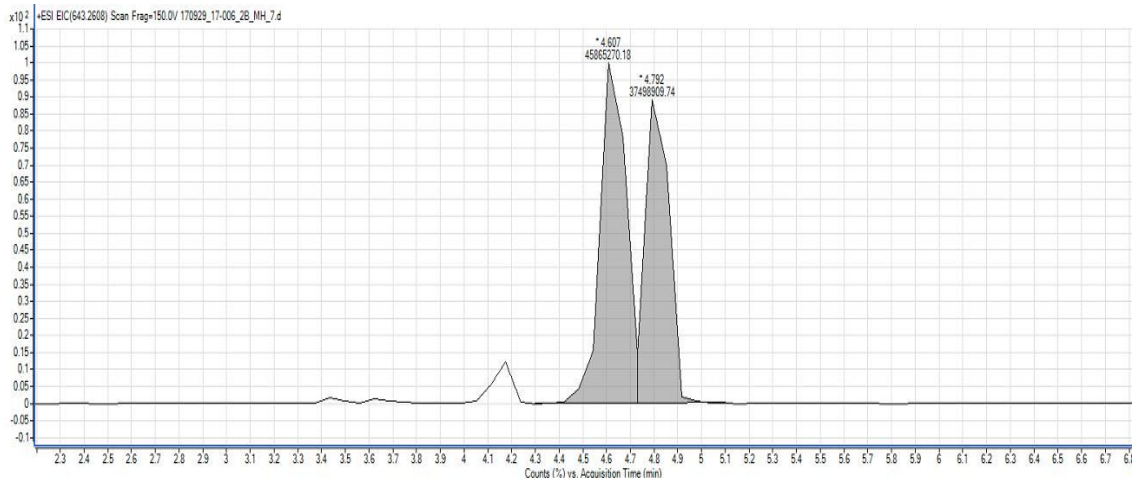

Figure S2J. Extracted ion chromatogram (EIC) of Barley Coleoptile.

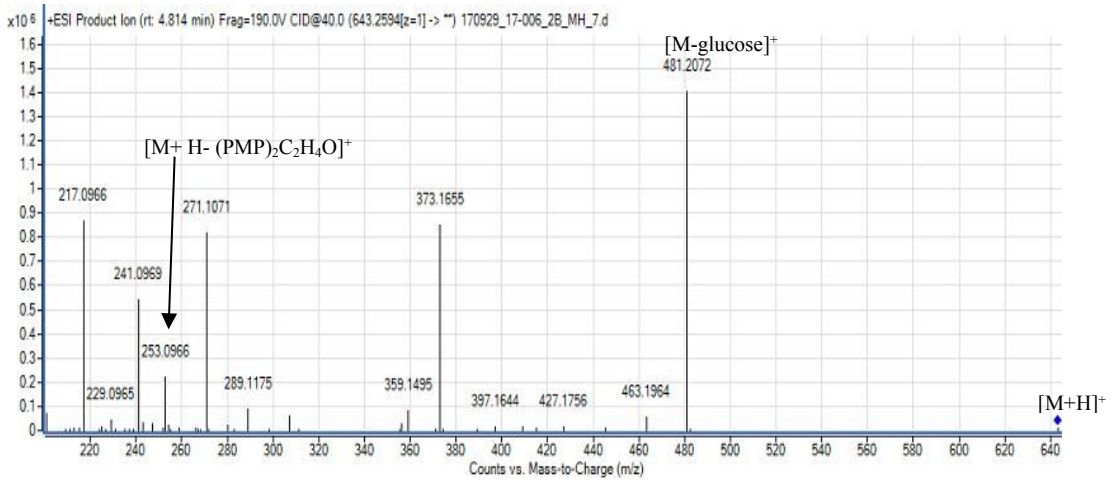

Figure S2K. Positive ESI-MS2 spectra of the $[M+ H]^+$ of PMP labeled Glc-(1,4)-β-Xyl disaccharide in Barley Coleoptile.

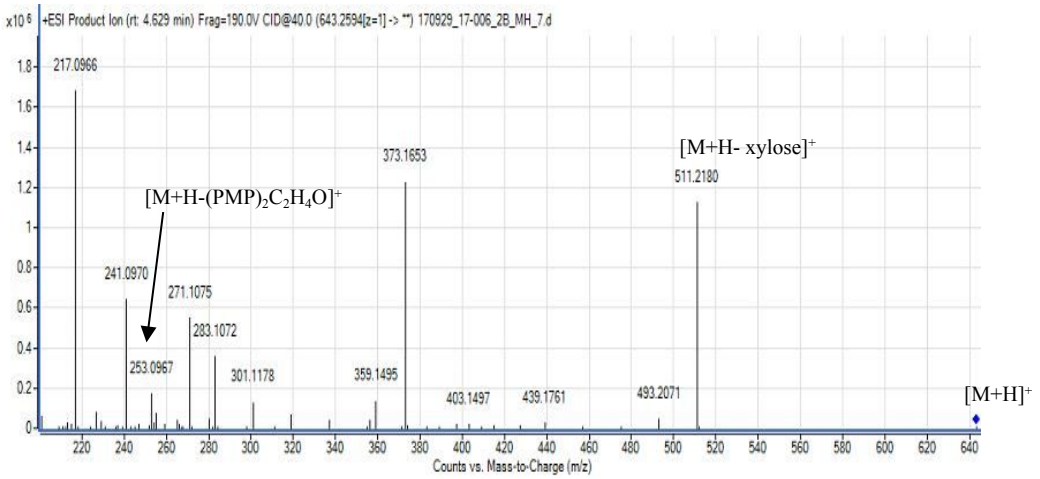

Figure S2L. Positive ESI-MS2 spectra of the [M+ H]$^+$ of PMP labeled Xyl-(1,4)-β-Glc disaccharide in Barley Coleoptile.

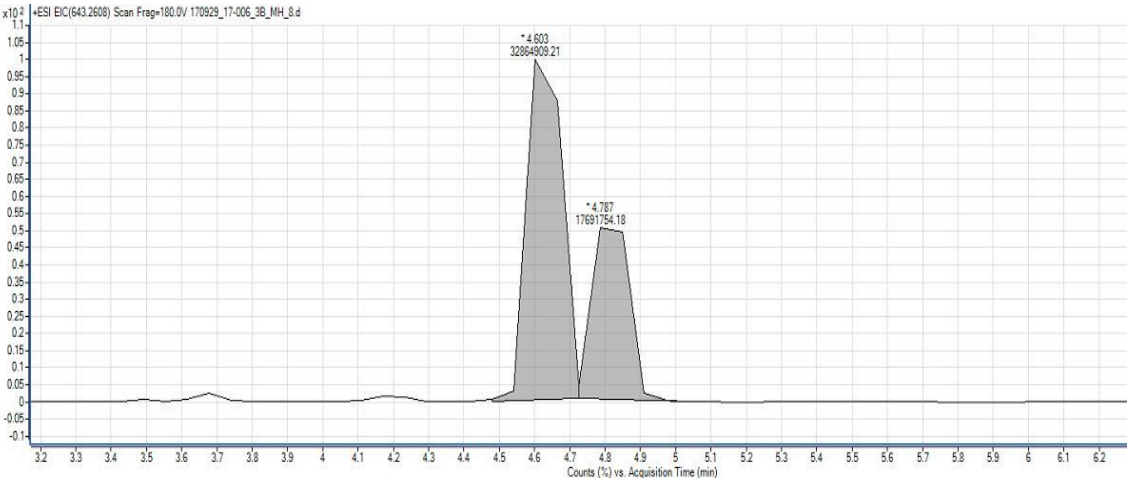

Figure S2M. Extracted ion chromatogram (EIC) of Barley Upper roots.

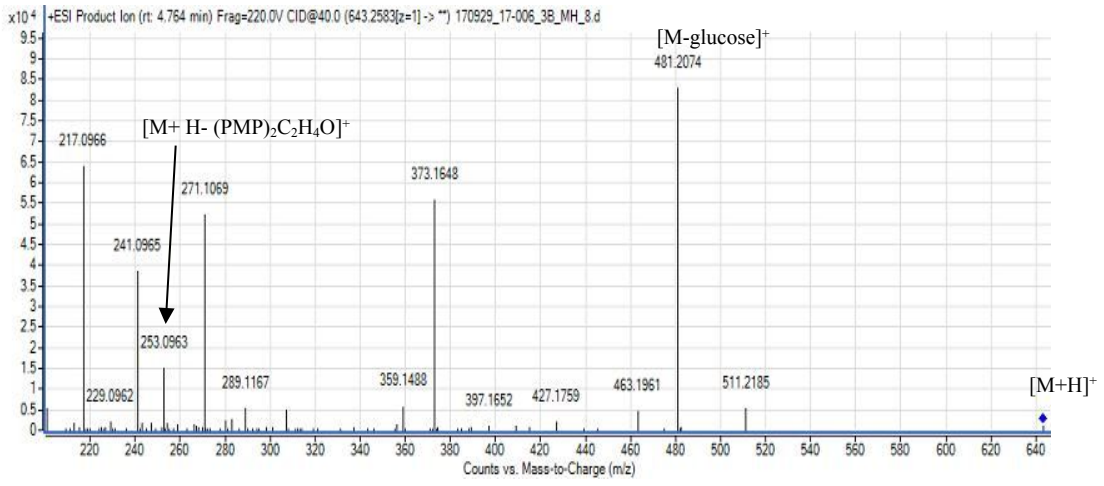

Figure S2N. Positive ESI-MS2 spectra of the [M+ H]$^+$ of PMP labeled Glc-(1,4)-β-Xyl disaccharide in Barley Upper roots.

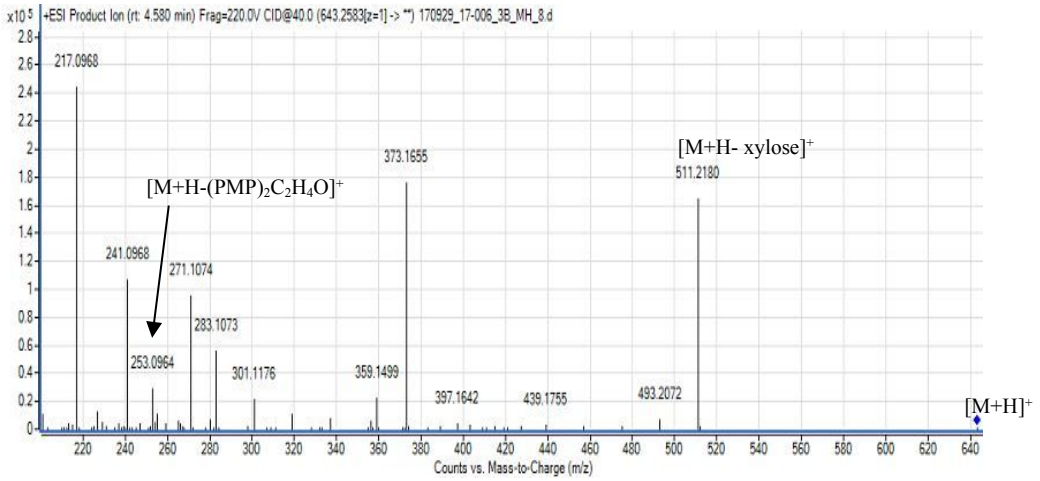

Figure S2O. Positive ESI-MS2 spectra of the $[M+ H]^+$ of PMP labeled Xyl-(1,4)-β-Glc disaccharide in Barley Upper roots.

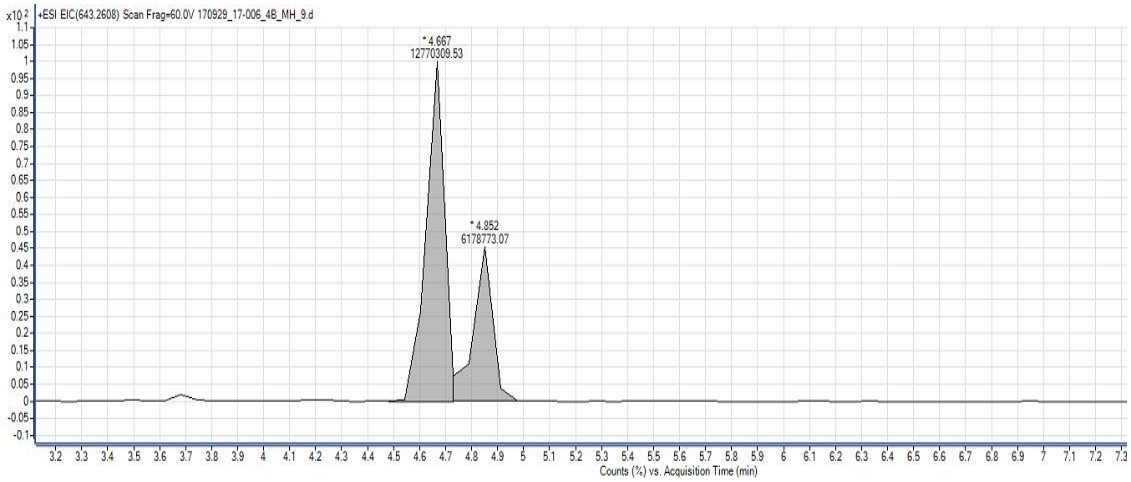

Figure S2P. Extracted ion chromatogram (EIC) of Barley Mid roots.

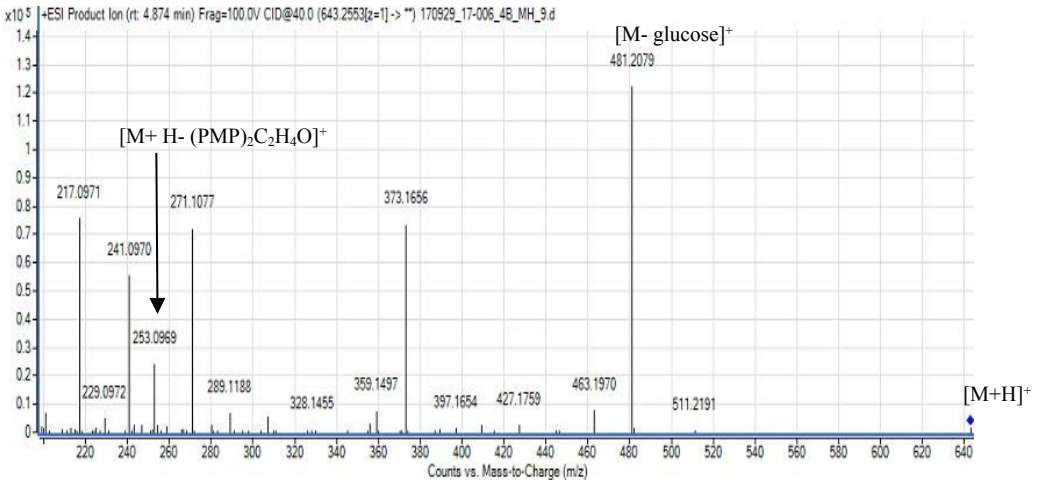

Figure S2Q. Positive ESI-MS2 spectra of the $[M+ H]^+$ of PMP labeled Glc-(1,4)-β-Xyl disaccharide in Barley Mid roots.

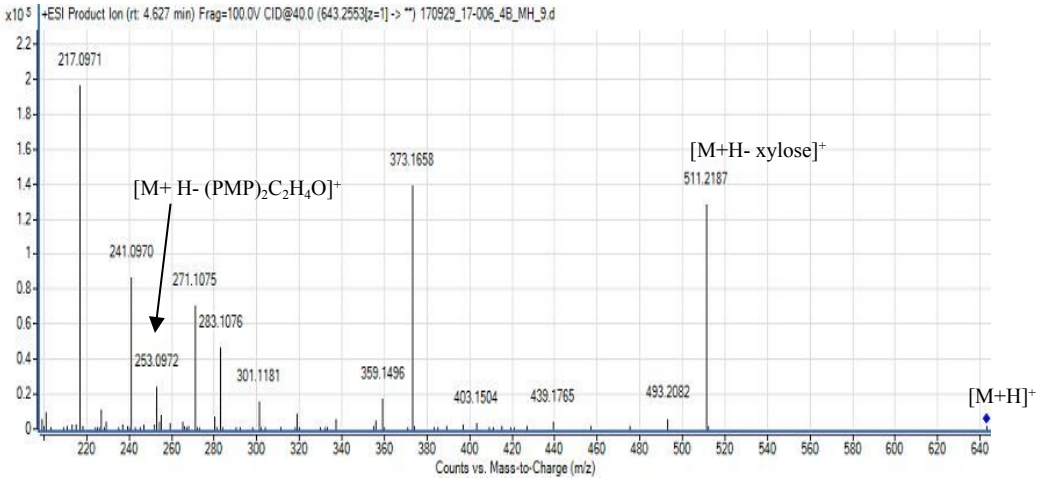

Figure S2R. Positive ESI-MS2 spectra of the $[M+ H]^+$ of PMP labeled Xyl-(1,4)-β-Glc disaccharide in Barley Mid roots.

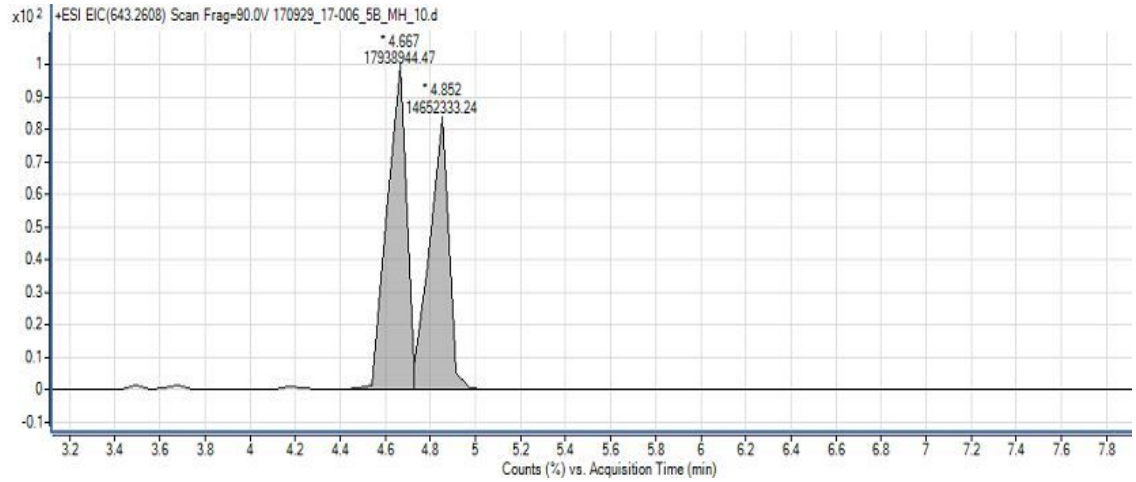

Figure S2S. Extracted ion chromatogram (EIC) of Barley Root tips.

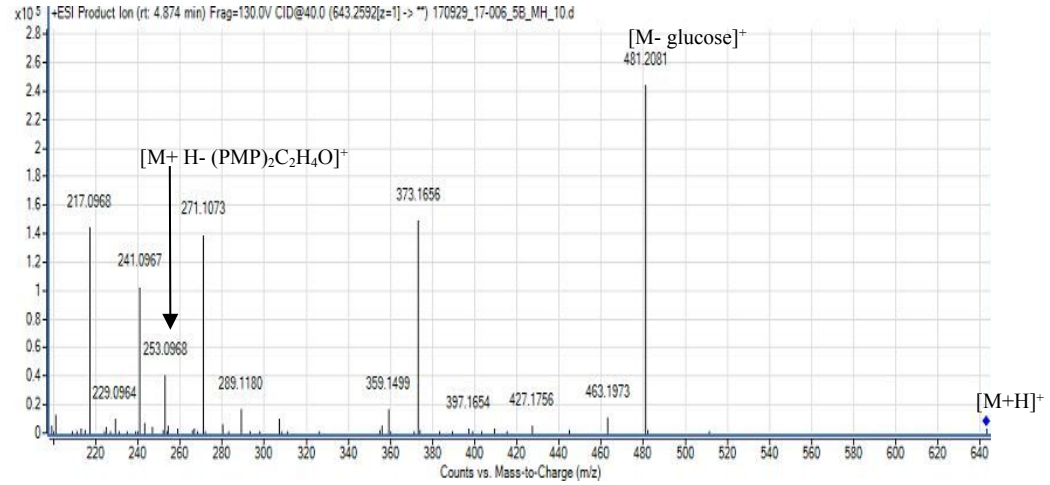

Figure S2T. Positive ESI-MS2 spectra of the $[M+ H]^+$ of PMP labeled Glc-(1,4)-β-Xyl disaccharide in Barley Root tips.

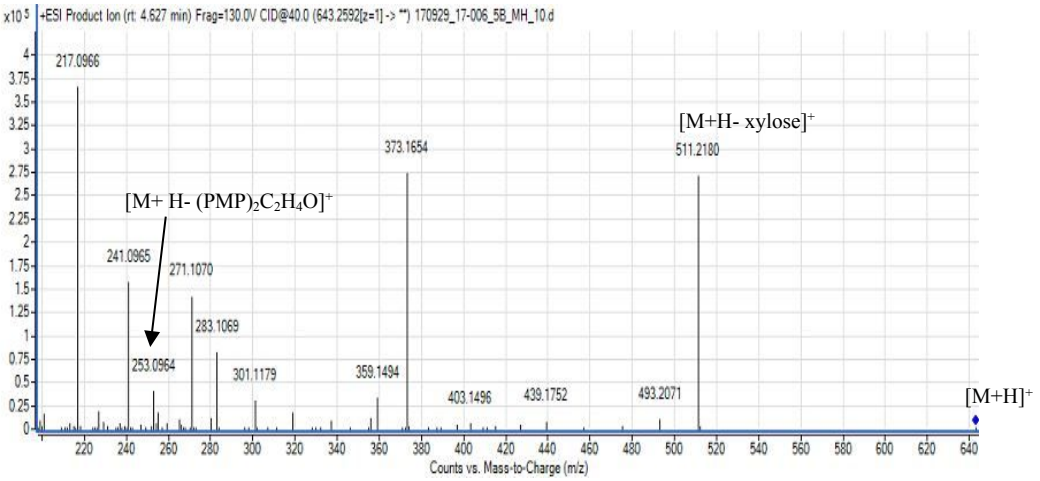

Figure S2U. Positive ESI-MS2 spectra of the $[M+ H]^+$ of PMP labeled Xyl-(1,4)-β-Glc disaccharide in Barley Root tips.

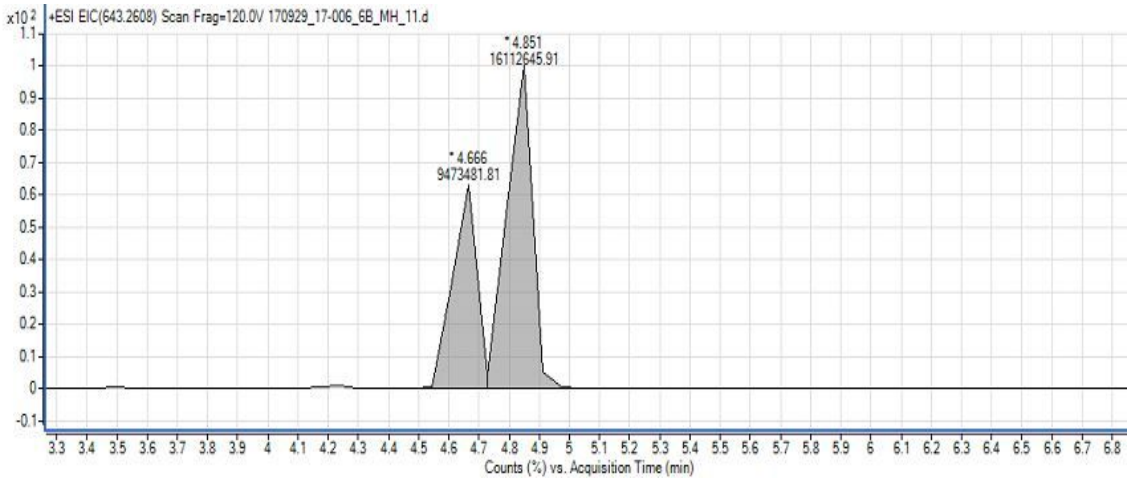

Figure S2V. Extracted ion chromatogram (EIC) of *Nicotiana benthamiana* negative control.

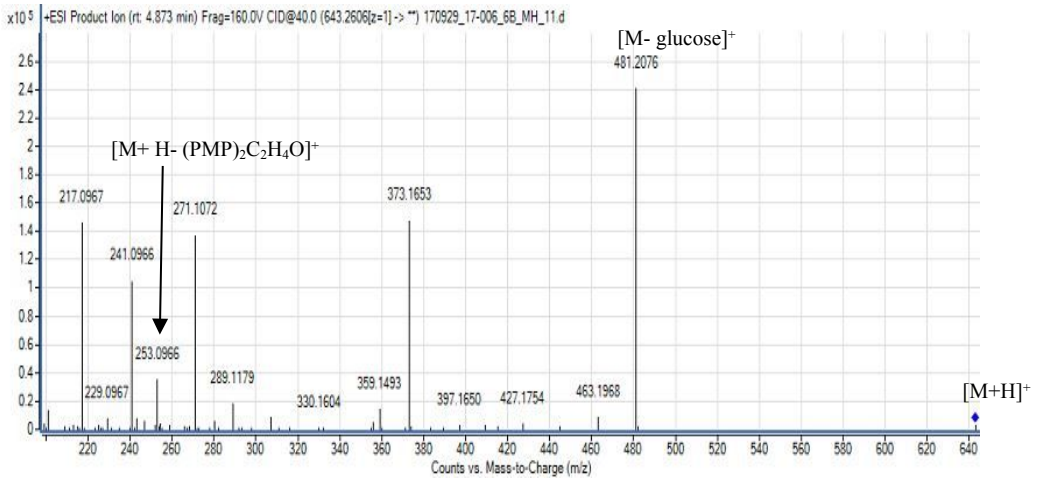

Figure S2W. Positive ESI-MS2 spectra of the $[M+ H]^+$ of PMP labeled Glc-(1,4)-β-Xyl disaccharide in *Nicotiana benthamiana* negative control.

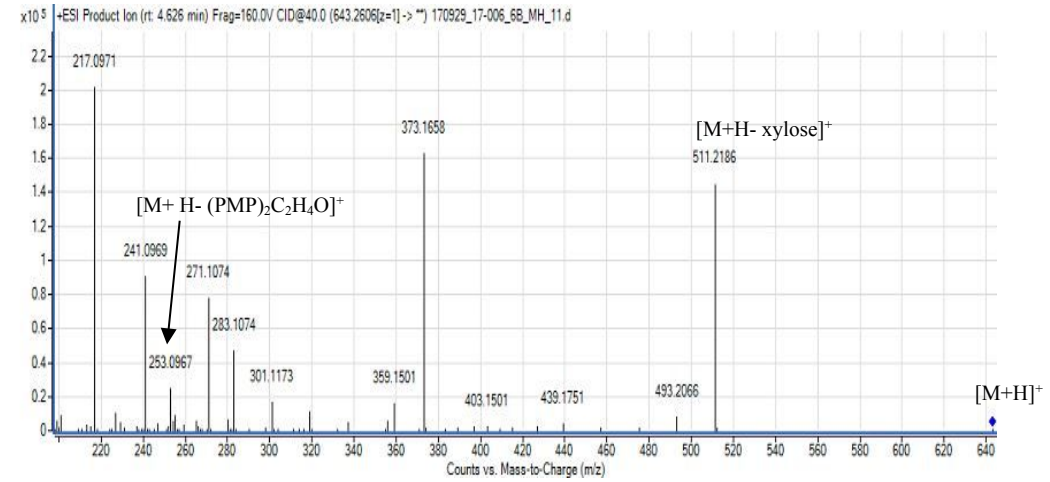

Figure S2X. Positive ESI-MS2 spectra of the $[M+ H]^+$ of PMP labeled Xyl-(1,4)-β-Glc disaccharide in *Nicotiana benthamiana* negative control.

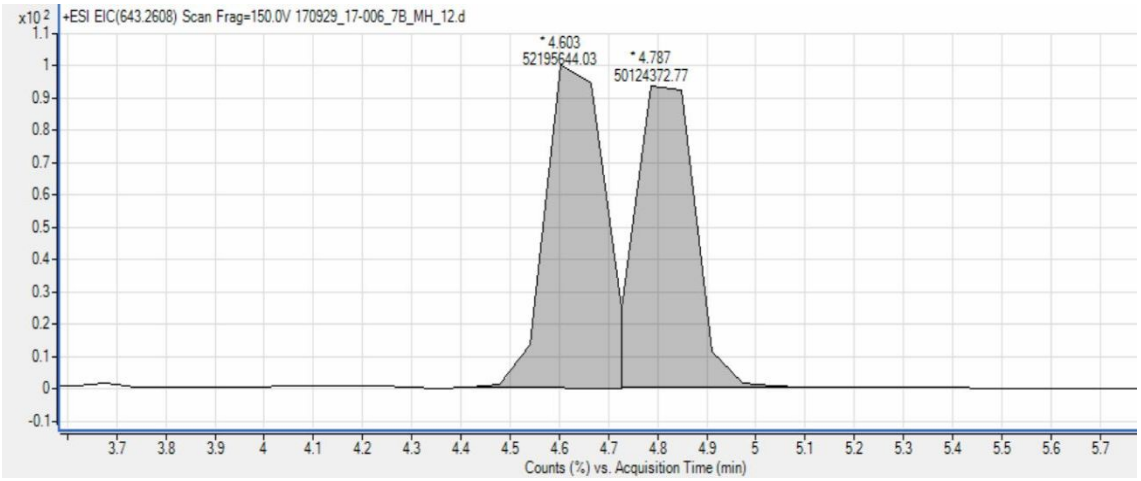

Figure S2Y. Extracted ion chromatogram (EIC) of *Nicotiana benthamiana* expressing *HvCslF3*.

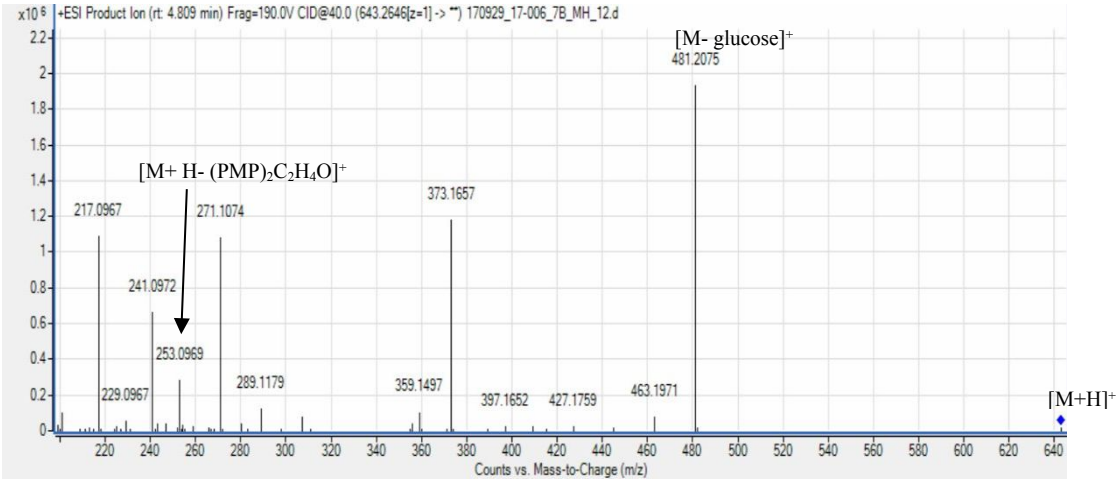

Figure S2Z. Positive ESI-MS2 spectra of the $[M+ H]^+$ of PMP labeled Glc-(1,4)-β-Xyl disaccharide in *Nicotiana benthamiana* expressing *HvCslF3*.

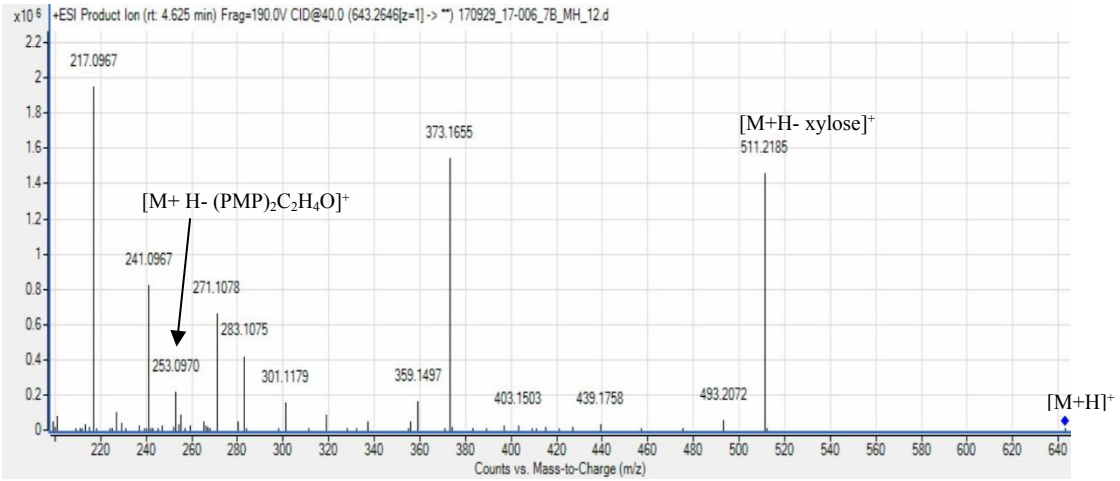

Figure S2AA. Positive ESI-MS2 spectra of the [M+ H]$^+$ of PMP labeled Xyl-(1,4)-β-Glc disaccharide in *Nicotiana benthamiana* expressing *HvCslF3*.

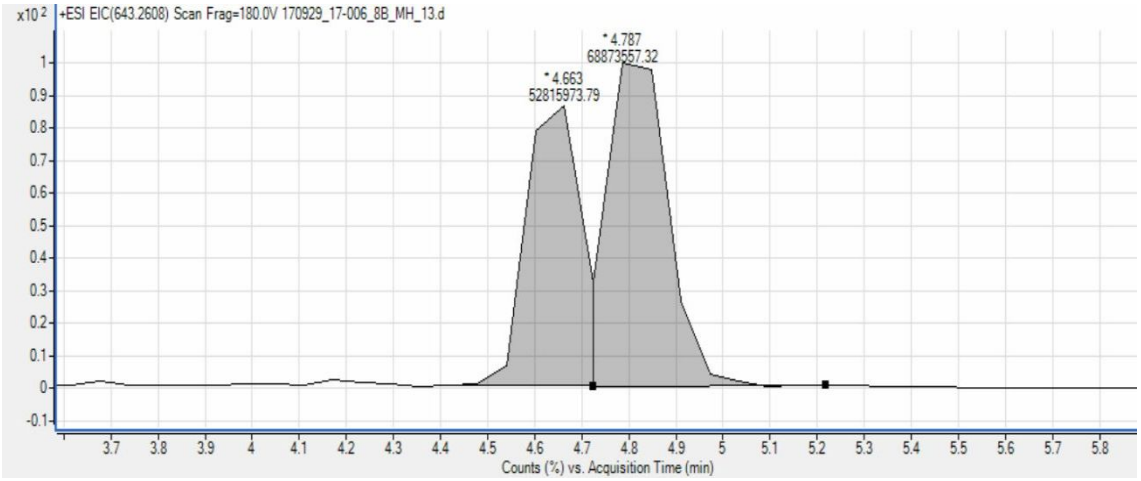

Figure S2BB. Extracted ion chromatogram (EIC) of *Nicotiana benthamiana* expressing *HvCslF10*.

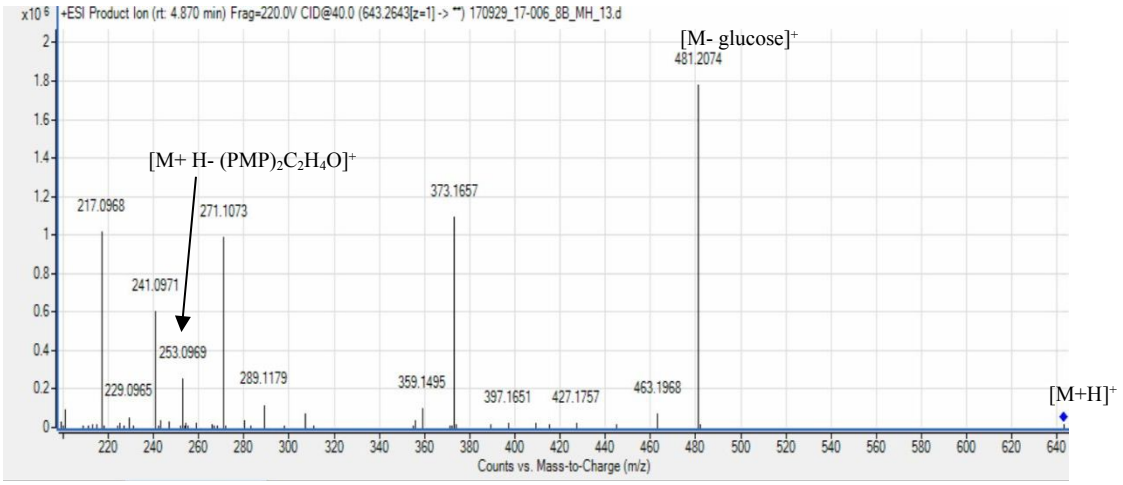

Figure S2CC. Positive ESI-MS2 spectra of the [M+ H]$^+$ of PMP labeled Glc-(1,4)-β-Xyl disaccharide in *Nicotiana benthamiana* expressing *HvCslF10*.

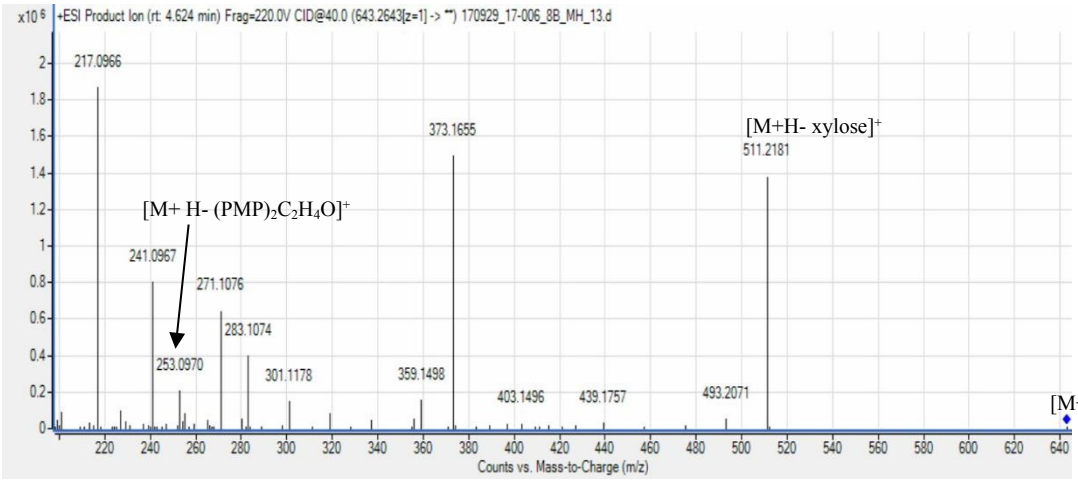

Figure S2DD. Positive ESI-MS2 spectra of the $[M+ H]^+$ of PMP labeled Xyl-(1,4)-β-Glc disaccharide in *Nicotiana benthamiana* expressing *HvCslF10*.

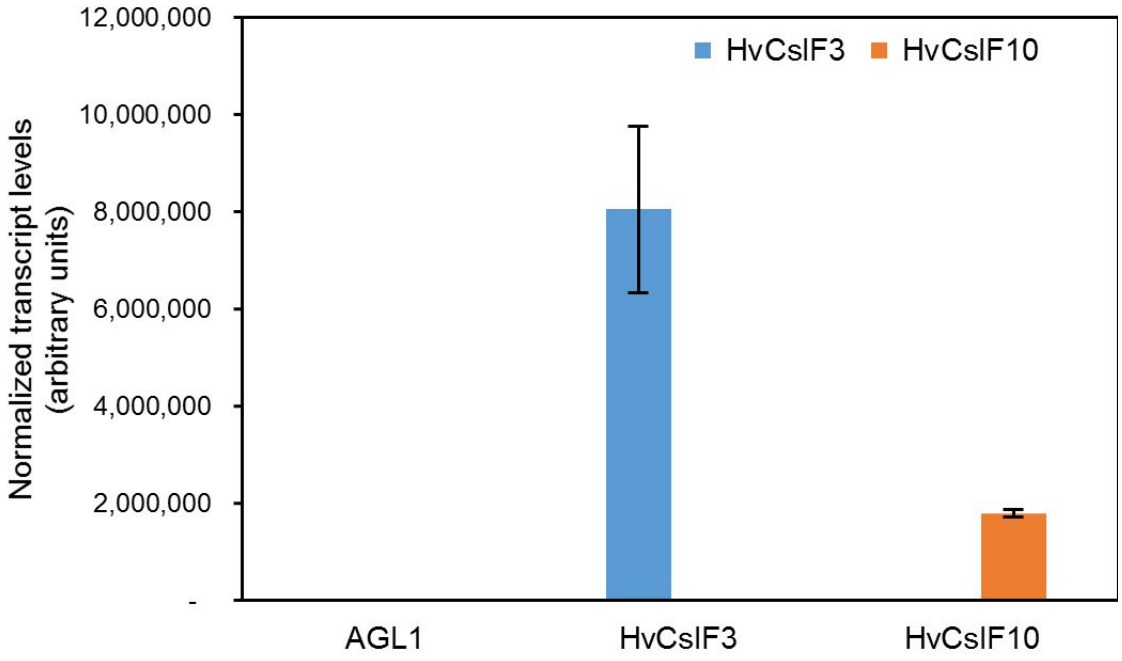

Supplementary Figure S3: Normalized transcript levels of *HvCslF3* and *HvCslF10* genes following heterologous expression in *N. benthamiana*. Error bars indicate standard deviation.

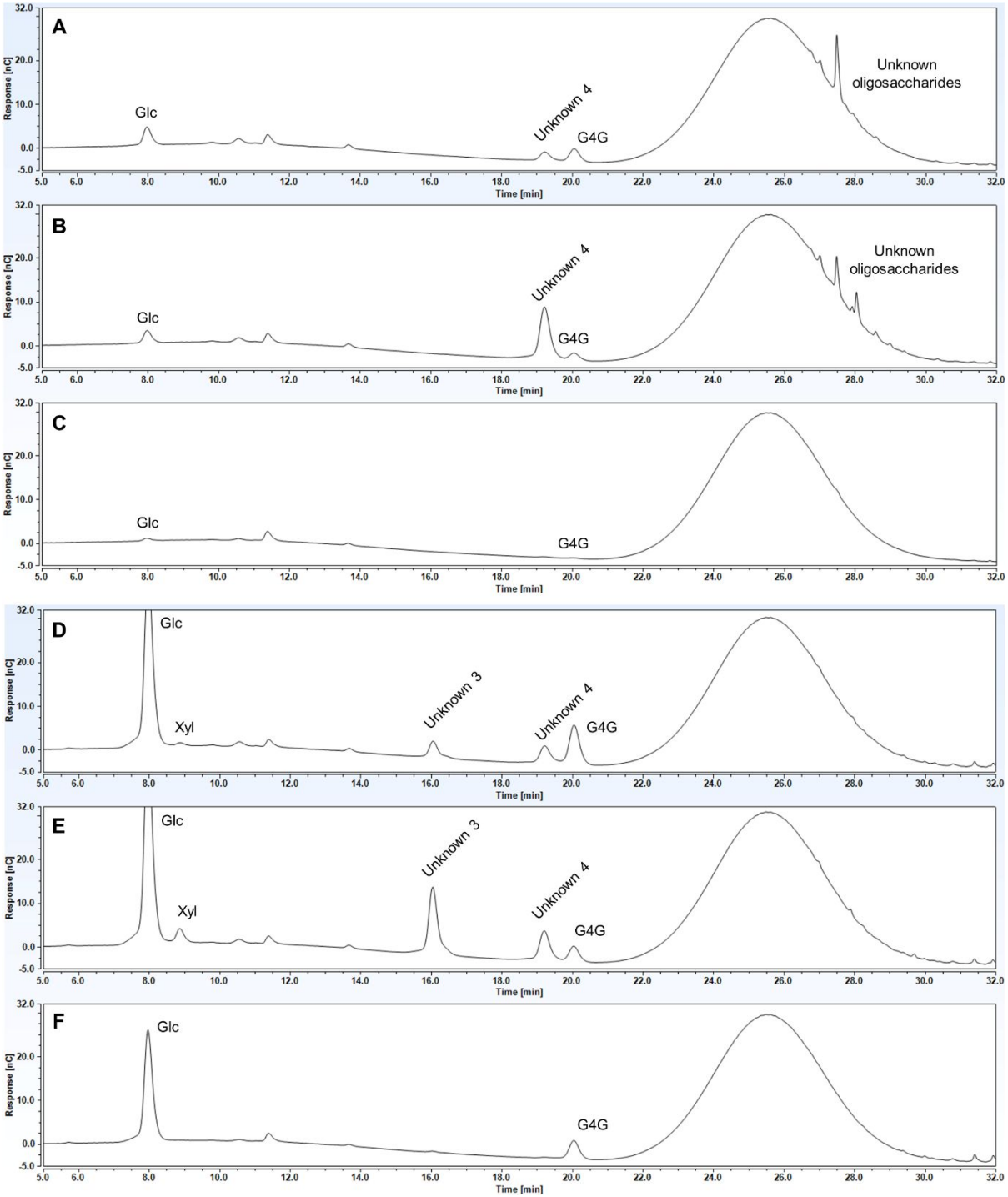

Supplementary Figure S4: Original HPAEC-PAD traces of oligosaccharides produced post-hydrolysis with cellulolytic enzymes of *N. benthamiana* leaf tissue overexpressing of *HvCslF3* and *HvCslF10*. Oligosaccharides released from *HvCslF3* (A), *HvCslF10* (B) expressing tissue and the empty vector control (C) by a cellulase from *Aspergillus niger* (E-CELAN), which has a preference for (1,4)-β-linkages in cellulose and (1,3;1,4)-β-glucan. Oligosaccharides released from *HvCslF3* (D), *HvCslF10* (E) expressing tissue and the empty vector control (F) by a cellulase from *Trichoderma longibrachium* (E-CELTR), which has a broader specificity.

Unknown 3 and 4 refer to peaks identified for further characterisation. x-axis: time, y-axis: abundance.

Supplementary Figure S5: LC-TOF MS analysis of oligosaccharides produced post-cellulase (E-CELAN) hydrolysis of *Nicotiana benthamiana* leaves expressing *HvCslF3* and *HvCslF10*. Two fractions of oligosaccharides eluting after XG and GX on HPAEC-PAD were prepared using Carbon SPE (Bond Elut 1mL / 50mg Agilent Technologies, Singapore). Monosaccharides and disaccharides were eluted with acetonitrile in water up to 10%, then 15% acetonitrile and 55% acetonitrile fractions were collected containing the larger oligosaccharides. These fractions were analyzed using HPAEC-PAD, monosaccharide analysis, and LC-MS^2 as their PMP derivatives.

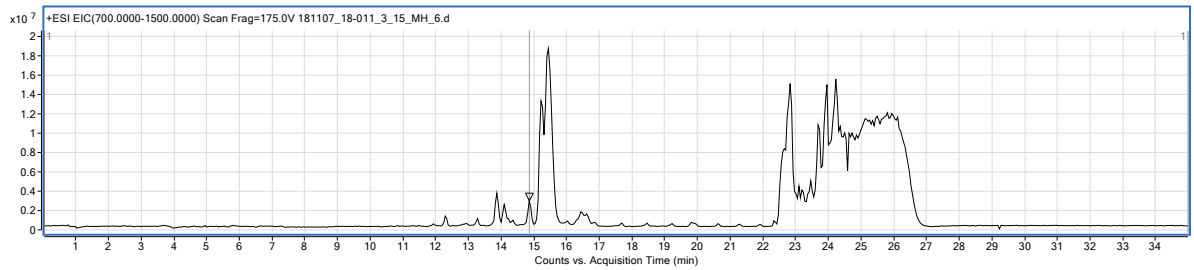

Figure S5A. Extracted ion chromatogram (EIC) of the 15% acetonitrile oligosaccharide fraction from *Nicotiana benthamiana* leaves expressing *HvCslF3*.

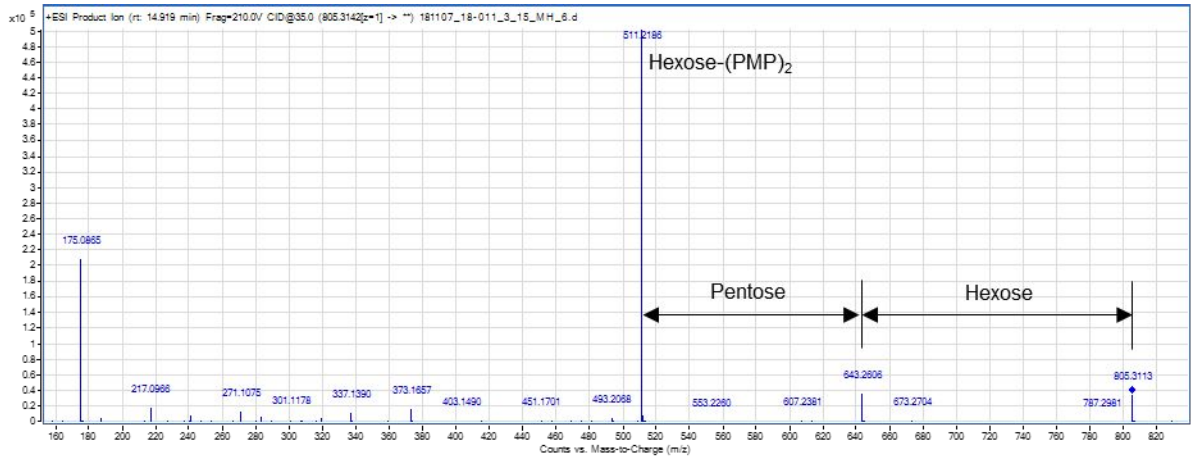

Figure S5B. Positive ESI-MS2 spectra of the $[M+H]^+$ of PMP labelled Glc-(1,4)-β-Xyl-(1,4)-β-Glc oligosaccharide indicated by arrow in Figure S5A.

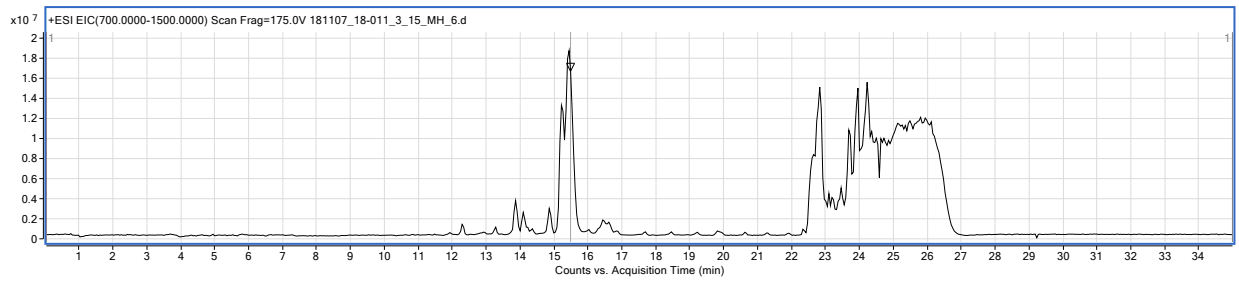

Figure S5C. Extracted ion chromatogram (EIC) of the 15% acetonitrile oligosaccharide fraction from *Nicotiana benthamiana* leaves expressing *HvCslF3*.

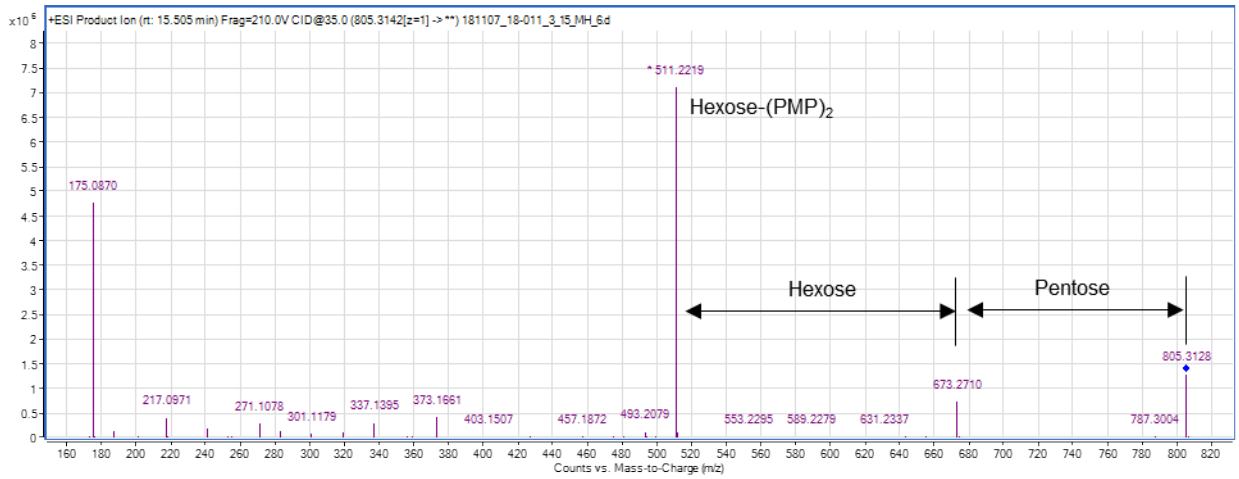

Figure S5D. Positive ESI-MS2 spectra of the $[M+H]^+$ of PMP labelled Xyl-(1,4)-β-Glc-(1,4)-β-Glc oligosaccharide indicated by arrow in Figure S5C.

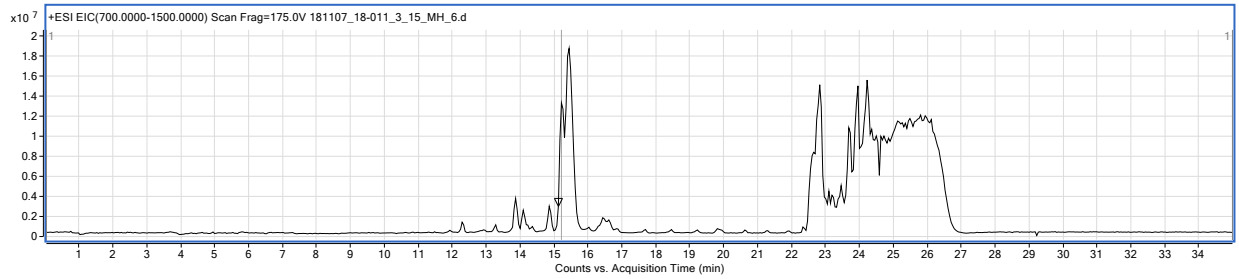

Figure S5E. Extracted ion chromatogram (EIC) of the 15% acetonitrile oligosaccharide fraction from *Nicotiana benthamiana* leaves expressing *HvCslF3*.

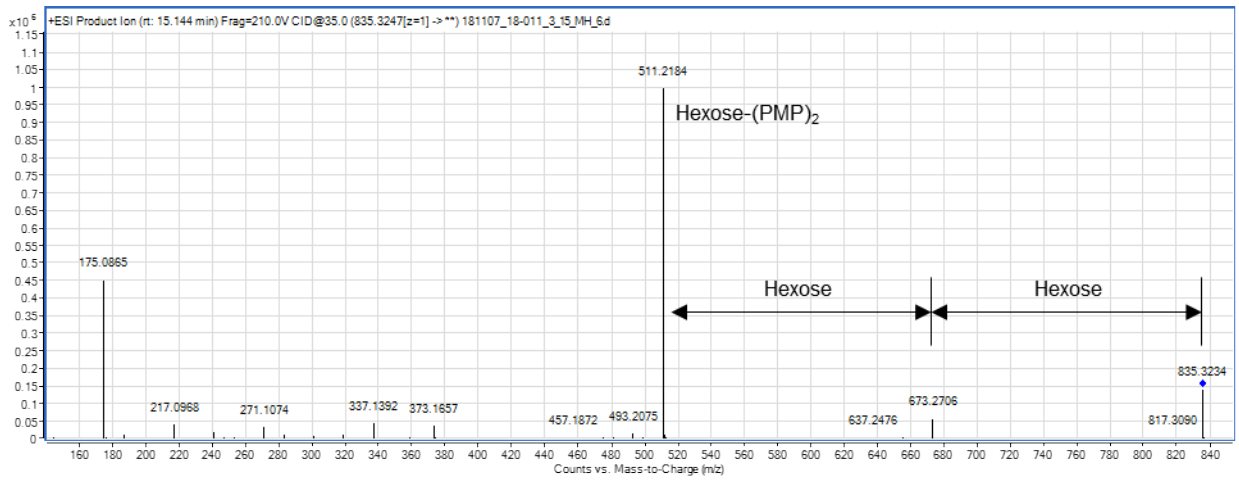

Figure S5F. Positive ESI-MS2 spectra of the $[M+H]^+$ of PMP labelled Glc-(1,4)-β-Glc-(1,4)-β-Glc oligosaccharide indicated by arrow in Figure S5E.

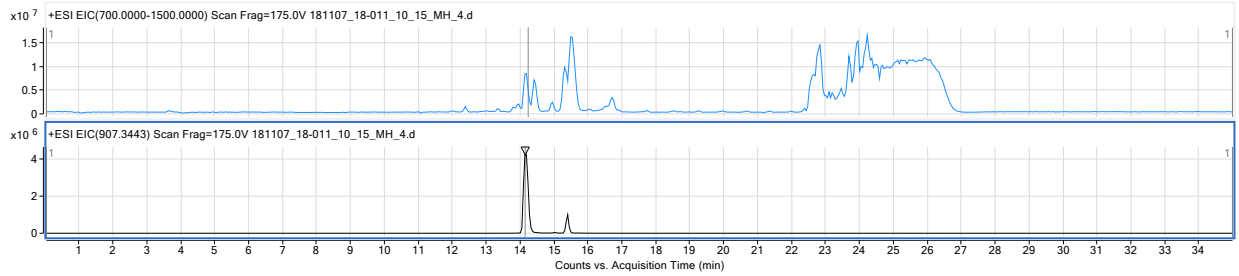

Figure S5G. Extracted ion chromatogram (EIC) of the 15% acetonitrile oligosaccharide fraction from *Nicotiana benthamiana* leaves expressing *HvCslF10*.

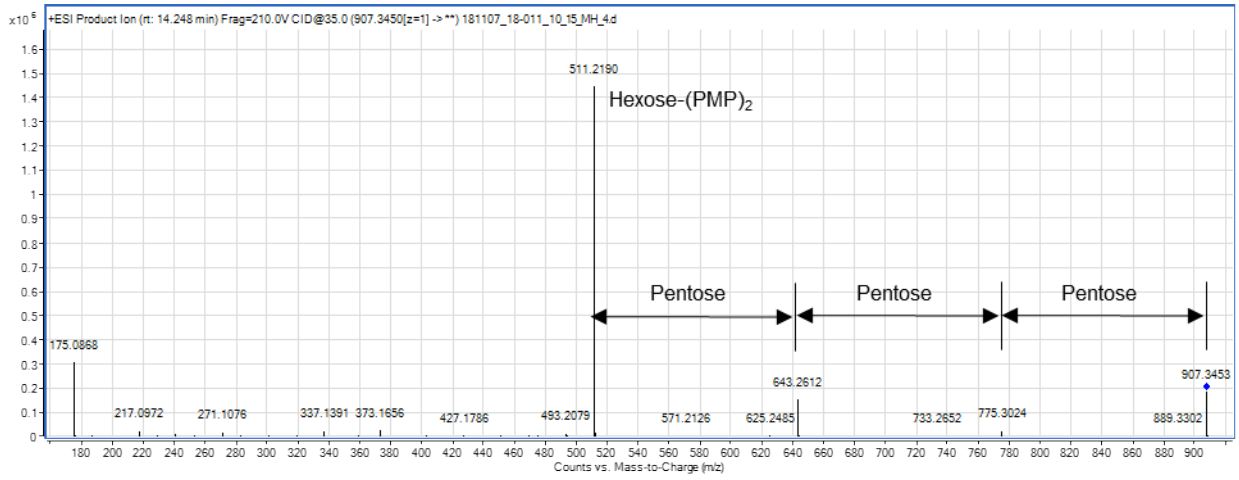

Figure S5H. Positive ESI-MS2 spectra of the $[M+H]^+$ of PMP labelled Xyl-(1,4)-β-Xyl-(1,4)-β-Xyl-(1,4)-β-Glc oligosaccharide indicated by arrow in Figure S5C.

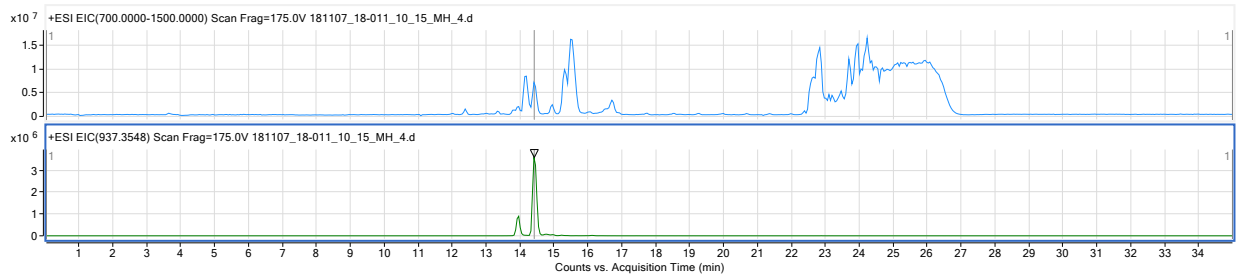

Figure S5I. Extracted ion chromatogram (EIC) of the 15% acetonitrile oligosaccharide fraction from *Nicotiana benthamiana* leaves expressing *HvCslF10*.

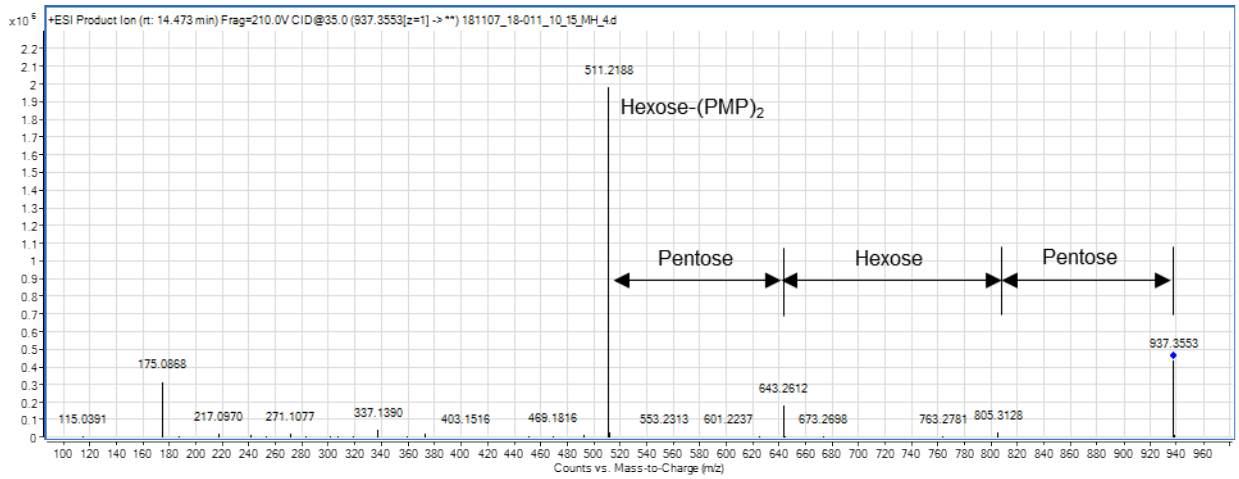

Figure S5J. Positive ESI-MS2 spectra of the $[M+H]^+$ of PMP labelled Xyl-(1,4)-β-Glc-(1,4)-β-Xyl-(1,4)-β-Glc oligosaccharide indicated by arrow in Figure S5I.

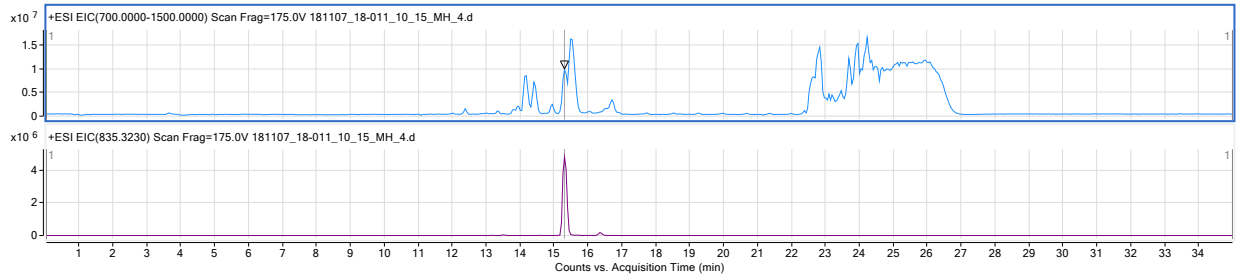

Figure S5K. Extracted ion chromatogram (EIC) of the 15% acetonitrile oligosaccharide fraction from *Nicotiana benthamiana* leaves expressing *HvCslF10*.

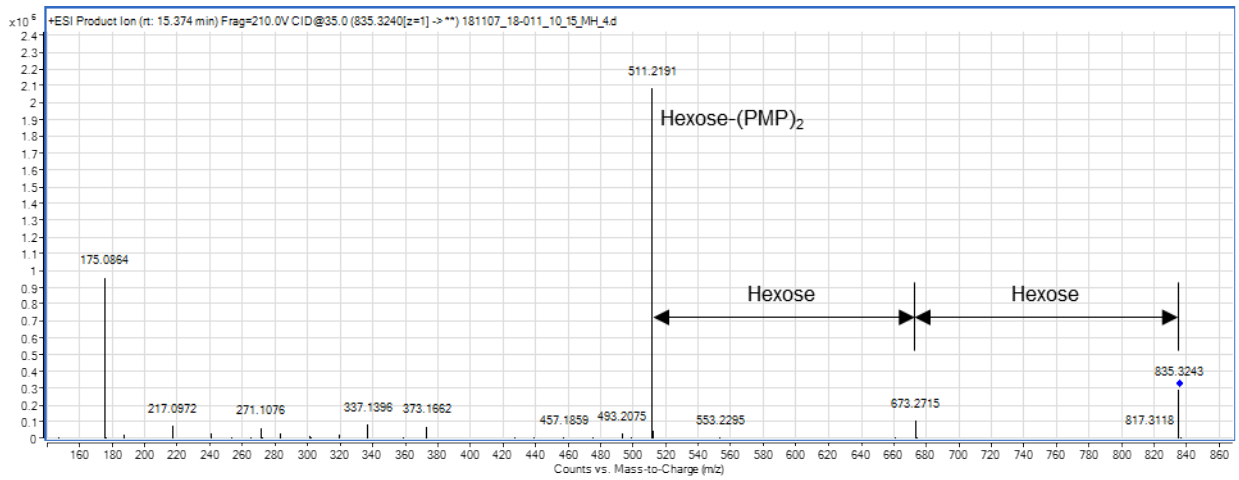

Figure S5L. Positive ESI-MS2 spectra of the $[M+H]^+$ of PMP labelled Glc-(1,4)-β-Glc-(1,4)-β-Glc oligosaccharide indicated by arrow in Figure S5K.

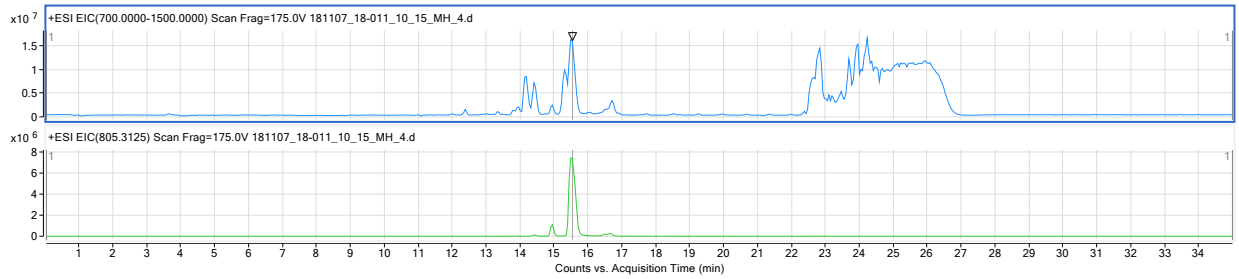

Figure S5M. Extracted ion chromatogram (EIC) of the 15% acetonitrile oligosaccharide fraction from *Nicotiana benthamiana* leaves expressing *HvCslF10*.

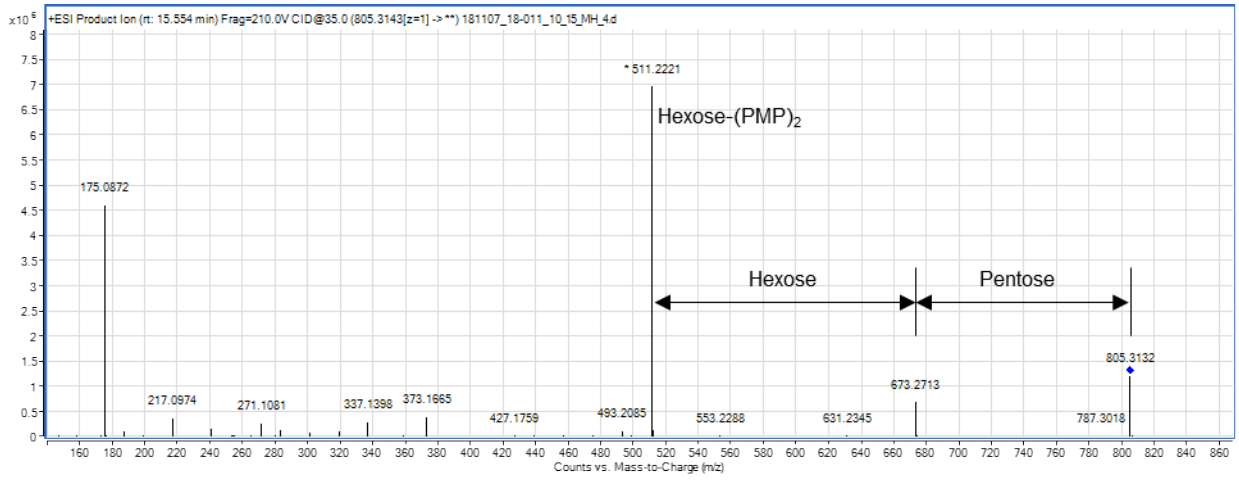

Figure S5N. Positive ESI-MS2 spectra of the $[M+H]^+$ of PMP labelled Xyl-(1,4)-β-Glc-(1,4)-β-Glc oligosaccharide indicated by arrow in Figure S5M.

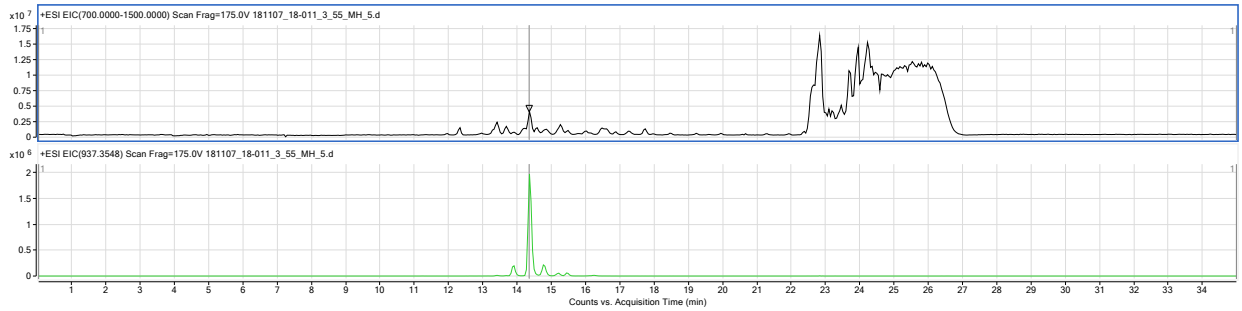

Figure S5O. Extracted ion chromatogram (EIC) of the 55% acetonitrile oligosaccharide fraction from *Nicotiana benthamiana* leaves expressing *HvCslF3*.

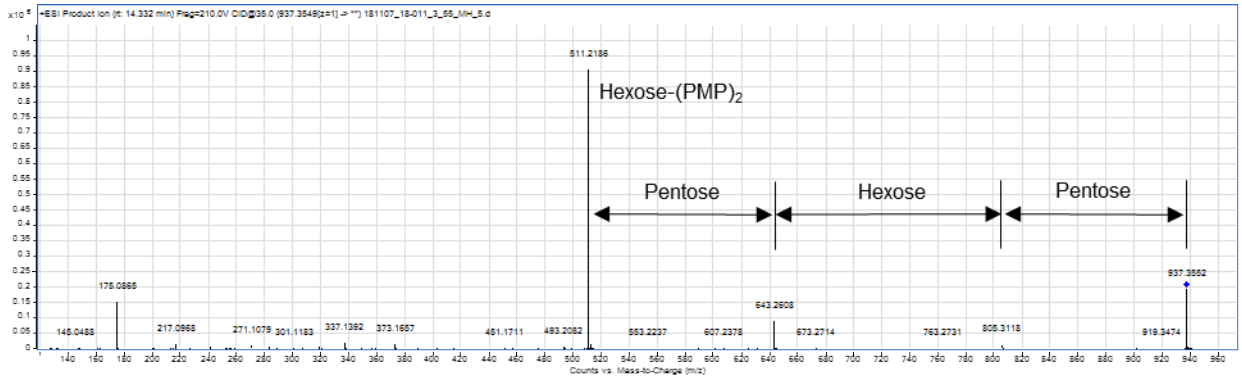

Figure S5P. Positive ESI-MS2 spectra of the $[M+H]^+$ of PMP labelled Xyl-(1,4)-β-Glc-(1,4)-β-Xyl-(1,4)-β-Glc oligosaccharide indicated by arrow in Figure S5O.

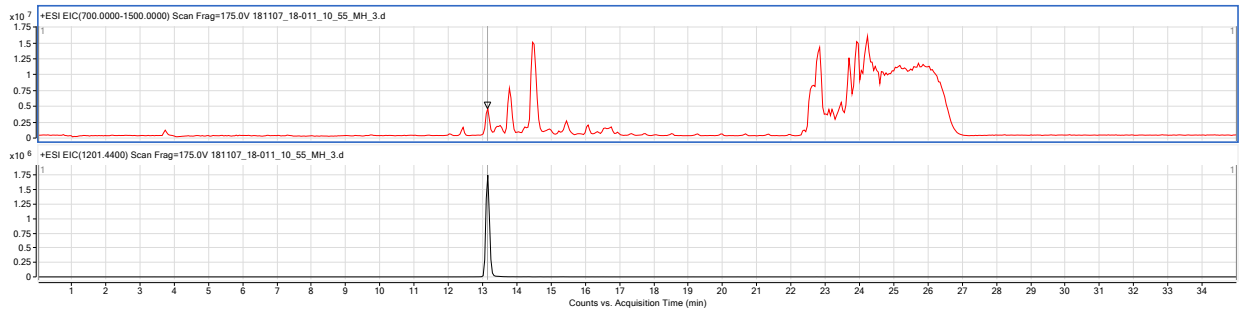

Figure S5Q. Extracted ion chromatogram (EIC) of the 55% acetonitrile oligosaccharide fraction from *Nicotiana benthamiana* leaves expressing *HvCslF10*.

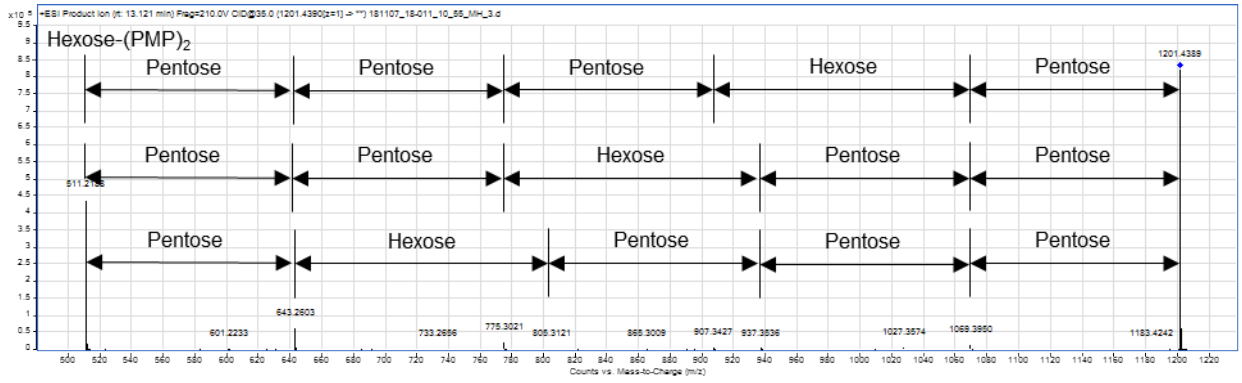

Figure S5R. Positive ESI-MS2 spectra of the $[M+H]^+$ of PMP labelled mixed hexamer oligosaccharides; Xyl-(1,4)-β-Glc-(1,4)-β-Xyl-(1,4)-β-Xyl-(1,4)-β-Xyl-(1,4)-β-Glc, Xyl-(1,4)-β-Xyl-(1,4)-β-Glc-(1,4)-β-Xyl-(1,4)-β-Xyl-(1,4)-β-Glc and Xyl-(1,4)-β-Xyl-(1,4)-β-Xyl-(1,4)-β-Glc-(1,4)-β-Xyl-(1,4)-β-Glc indicated by arrow in Figure S5Q.

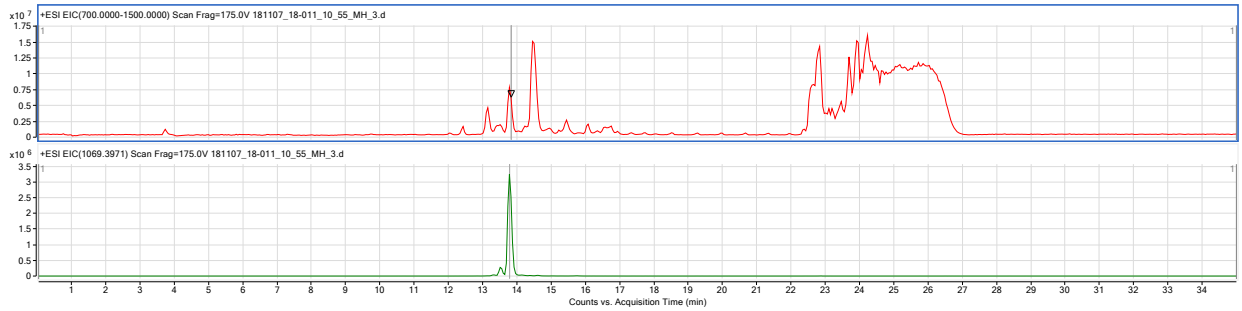

Figure S5S. Extracted ion chromatogram (EIC) of the 55% acetonitrile oligosaccharide fraction from *Nicotiana benthamiana* leaves expressing *HvCslF10*.

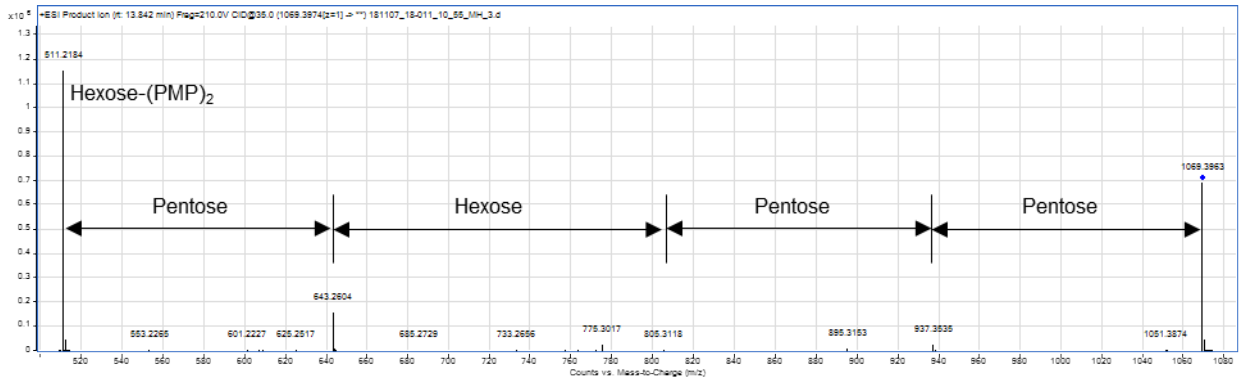

Figure S5T. Positive ESI-MS2 spectra of the $[M+H]^+$ of PMP labelled Xyl-(1,4)-β-Xyl-(1,4)-β-Glc-(1,4)-β-Xyl-(1,4)-β-Glc oligosaccharide indicated by arrow in Figure S5S.

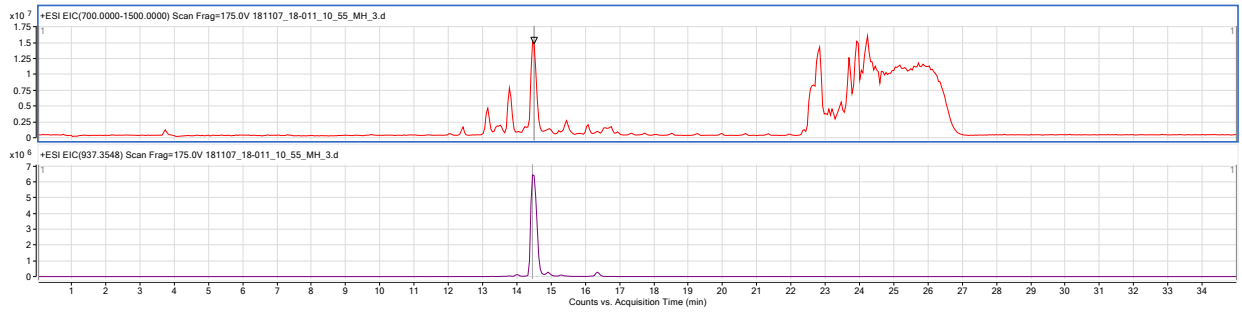

Figure S5U. Extracted ion chromatogram (EIC) of the 55% acetonitrile oligosaccharide fraction from *Nicotiana benthamiana* leaves expressing *HvCslF10*.

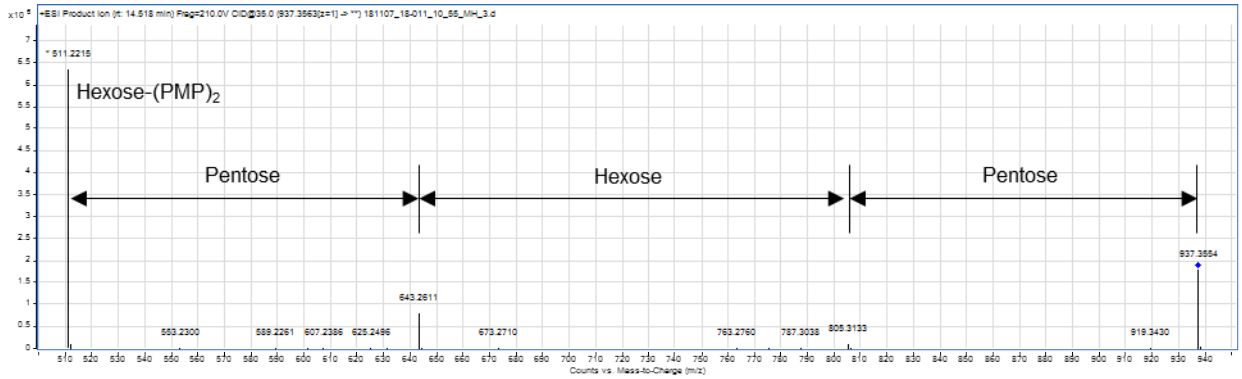

Figure S5V. Positive ESI-MS2 spectra of the $[M+H]^+$ of PMP labelled Xyl-(1,4)-β-Glc-(1,4)-β-Xyl-(1,4)-β-Glc oligosaccharide indicated by arrow in Figure S5U.

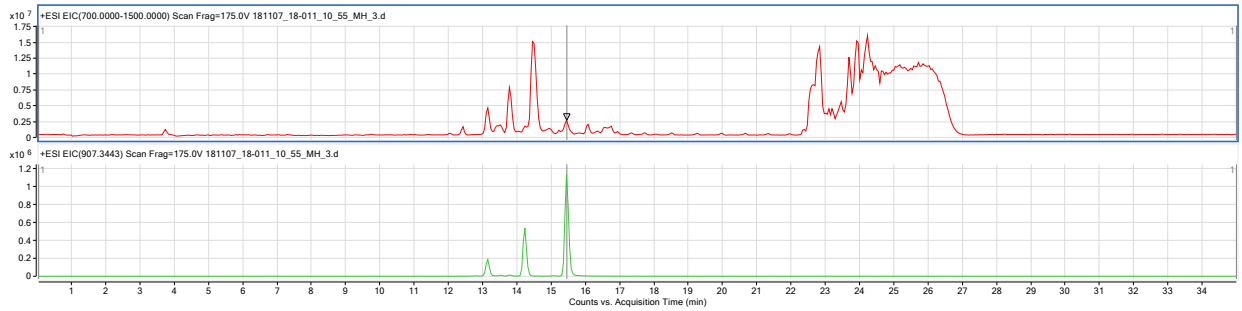

Figure S5W. Extracted ion chromatogram (EIC) of the 55% acetonitrile oligosaccharide fraction from *Nicotiana benthamiana* leaves expressing *HvCslF10*.

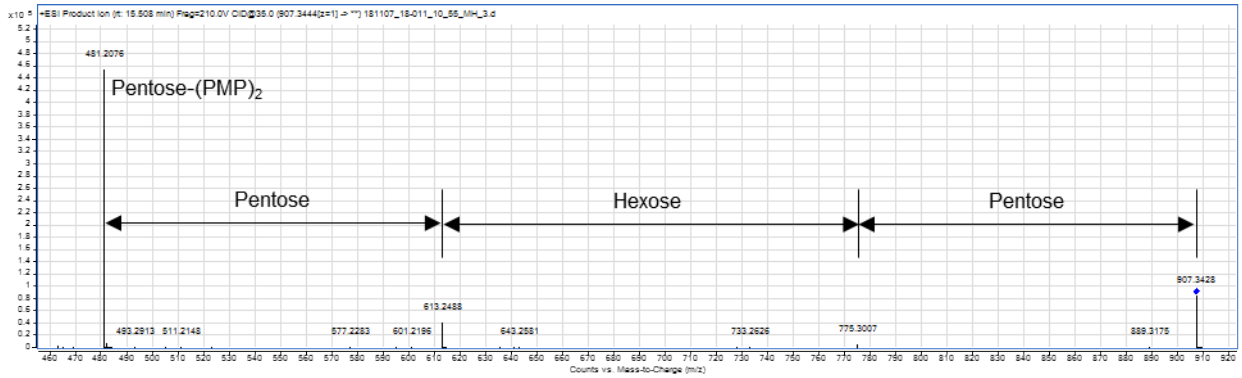

Figure S5X. Positive ESI-MS2 spectra of the $[M+H]^+$ of PMP labelled Xyl-(1,4)-β-Glc-(1,4)-β-Xyl-(1,4)-β-Xyl oligosaccharide indicated by arrow in Figure S5W.

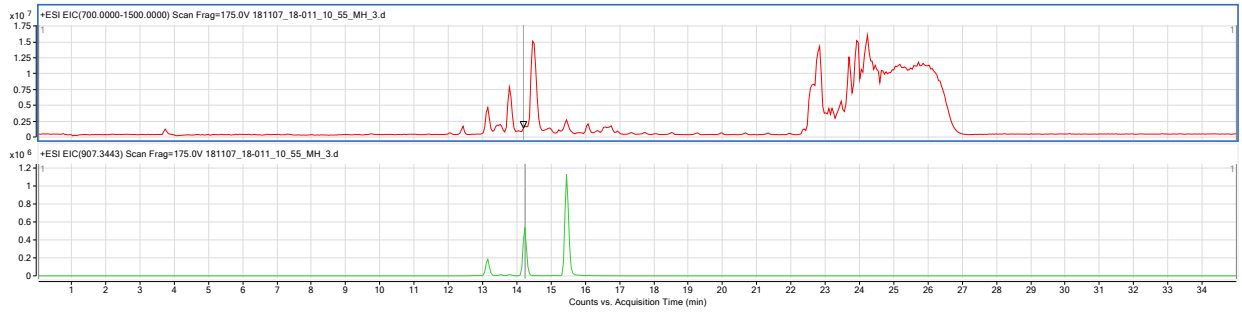

Figure S5Y. Extracted ion chromatogram (EIC) of the 55% acetonitrile oligosaccharide fraction from *Nicotiana benthamiana* leaves expressing *HvCslF10*.

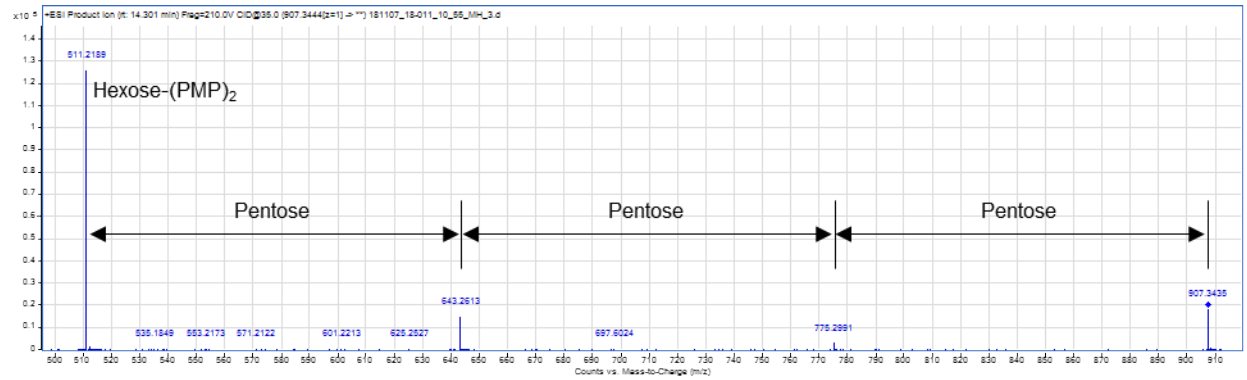

Figure S5Z. Positive ESI-MS2 spectra of the $[M+ H]^+$ of PMP labelled Xyl-(1,4)-β-Xyl-(1,4)-β-Xyl-(1,4)-β-Glc oligosaccharide indicated by arrow in Figure S5Y.